UNIVERSITY OF CALIFORNIA
RIVERSIDE

Particle Emissions From Vehicles (SI-PFI and SI-DI) at High Speed and From Large Ocean-Going Vessels

A Thesis submitted in partial satisfaction
of the requirements for the degree of

Master of Science

in

Chemical and Environmental Engineering

by

Carlos Espinoza

December 2014

Thesis Committee:

Dr. Akua Asa-Awuku, Chairperson
Dr. David R Cocker III
Dr. Georgios Karavalakis

The Thesis of Carlos Espinoza is approved:

_____

_____

_____

Committee Chairperson

University of California, Riverside

ACKNOWLEDGEMENTS

First, I would like to express my deep and sincere gratitude to my advisor, Dr. Akua Asa-Awuku. She was more than an outstanding advisor, she has been an inspiration throughout my journey at UCR. She provided me with an open-door policy to give insightful guidance and continuous support throughout my studies. I was very fortunate to have had such a wonderful human being as an advisor. I would also like to thank my co-advisor Dr. David Cocker who provided the opportunity to discuss my progress through weekly group meetings. He gave great suggestions and guidelines on improving my work. Dr. Georgios Karavalakis was also an outstanding advisor. He helped me understand engine technologies, combustion, fuel properties, and trends in the data. Dr. Kent Johnson was also there to help guide me along the emissions world. He gave me the opportunity to work on real-world emissions testing, attend a conference to discuss our findings, and understand how to find meaning in data. Without their support, my interests in engineering and appreciation for the environment would not be what they are today. In addition, I would also like to thank the great team of researchers at CE-CERT whom I have had the privilege to work with, in particular: Dr. Daniel Short, Dr. Michael Giordano, Diep Vu, Vincent Chen and Ashely Vizenor. They were more than colleagues. We grew together to become close friends and encourage each other during times of hardship.

Lastly, I would like to thank my family who provided me continuous inspiration and support throughout my educational journey.

Thank you all.

ABSTRACT OF THE THESIS

Particle Emissions From Vehicles (SI-PFI and SI-DI) at High Speed and From Large Ocean-Going Vessels

by

Carlos Espinoza

Master of Science, Graduate Program in Chemical and Environmental Engineering
University of California, Riverside, December 2014
Dr. Akua Asa-Awuku, Chairperson

Light-duty passenger cars and large ocean-going vessels represent two particle emission sources that have the ability to affect human health, climate change and air quality in local communities and worldwide. Driving speed and engine technology are two factors that can affect vehicle emissions. In California, drivers can drive upwards of 70% at speeds above the posted limits. This can cause high uncertainty when modeling vehicle emissions. The first part of this thesis examines both high-speed driving and direct-injection effects on particle concentration and composition while the second part examines the effectiveness of a scrubber technology to remove particulate matter (PM) from large ocean-going vessel emissions. The results show that high-speed driving can affect both total particle count and composition significantly as well as direct-injection technology. Ocean-going vessels equipped with a scrubber are effective at removing gaseous SO_2, however, they are not as effective at removing PM or black carbon (BC).

Table of Contents

List of Figures

List of Tables

Particle Emissions From Spark Ignition Port-Fuel (SI-PFI) and Spark-Ignition Direct Injection Vehicles (SI-DI) at High Speed

1. Background

Policy makers are currently pressuring automobile manufacturers to meet stringent emission and efficiency standards in the United States. They are pressured to increase the average fleet fuel economy to 54.5 miles per gallon (mpg) by 2025[1]. As a result, automobile manufacturers are dynamically redesigning their gasoline light duty fleet. Such designs include adapting lighter construction materials such as aluminum and adapting different engine technologies such as gasoline-direct injection (GDI). These improve fuel economy by reducing gross vehicle weight and by precisely delivering fuel directly to the combustion chamber. GDI engine technology is expected to dominate 93% of market by 2025 [2]. GDI technology can offer up to 15% higher fuel economy and lower CO_2 yet particle number emissions remain highly misunderstood for GDI and PFI cars under high speed. Anthropogenic particle emissions are an important factor when considering this technology as they are a major contributor to local air pollution and global climate change[3]. More specifically, particle phase emissions are among the leading causes of respiratory illnesses and are even considered carcinogenic[4]. Particle emissions from this engine technology under high load have not been thoroughly assessed. Thus, this research aids to better understand the air pollution consequences of adapting this engine technology.

1.2 Vehicle Engine Technology

The continuous price increase trend with fuel prices necessitates the improvement of gasoline engines, there is a growing market demand for fuel efficient cars[5]. Car manufacturers have configured engines such that fuel economy can be increased through

the implementation of GDI. The two main factors attributed to engine efficiency include the compression ratio, and the air-fuel ratio. Higher compression ratios could lead engine knocking. Maximizing efficiency can be achieved by an air-fuel ratio that is lean[5]. PFI engines are designed to operate at stoichiometric air-fuel ratios and thus it is not possible to increase fuel economy with this approach. GDI engines however, can operate differently according to load. A GDI engine can operate with a lean air-fuel mixture during low loads and with a stoichiometric or slightly rich mixture at high loads[5]. In GDI engines, fuel is injected directly into the combustion chamber prior to ignition by the spark plug. During low or medium engine loads, the air fuel ratio can vary inside the combustion chamber, creating fuel rich zones and lean conditions simultaneously[5]. For example, the air-fuel mixture may be rich near the spark plug prior to ignition and lean elsewhere, this decreases fuel consumption and power output, thus is only programmed during low or medium load conditions. During high load conditions, homogeneous, or stoichiometric operation can take place. Fuel is injected at the intake stroke, evaporated and ignited. The evaporation of the fuel may increase volumetric efficiency by increasing the compression ratio up to 12:1[6] and ultimately higher torque. Because the fuel is directly injected into the combustion chamber either just prior to ignition or during the intake stroke the fuel must be injected at high pressure to help with the vaporization process. Even with high pressures, not all fuel has enough time to vaporize and can result in piston and wall wetting[6]. In return, incomplete combustion may occur the reaction is diffusion limited and oxygen may not reach all areas of the cylinder, leaving unburned fuel that ultimately turns to soot and increases particle pollution.

1.3 Driving speed trends and emissions modeling

In California, the California Air Resources Board (CARB) estimates emissions from on-road vehicles from the emission factor model (EMFAC). The model uses speed correction factors to adjust emission factors for speeds greater than 65 miles per hour (mph). The correction factors used are based on emission-versus-speed curve fittings of unified correction cycles whose speed values range from 5 to 65 mph. Strong evidence from the California Department of Transportation (Caltrans) Freeway Performance Measurement System (PEMS) suggests that more than 50% of freeway vehicle miles traveled (VMT) in California are at speeds above 65 mph. Furthermore, more than 40% of the total VMT in California occur on interstates and freeways, see Figures 1-3.1 and 1-3.2. Based on EMFAC 2011 model, it is clear that modeling vehicle emissions at high speed in California is still subject to large uncertainties. Inaccurate emission factors could be used when considering speeds greater than 65 mph and consequently mislead the design of countermeasures to control emissions as well as the benefits of GDI technology. Therefore, it is desirable to measure emissions from light-duty vehicles under speeds greater than 65 mph and ultimately supplement EMFAC 2011.

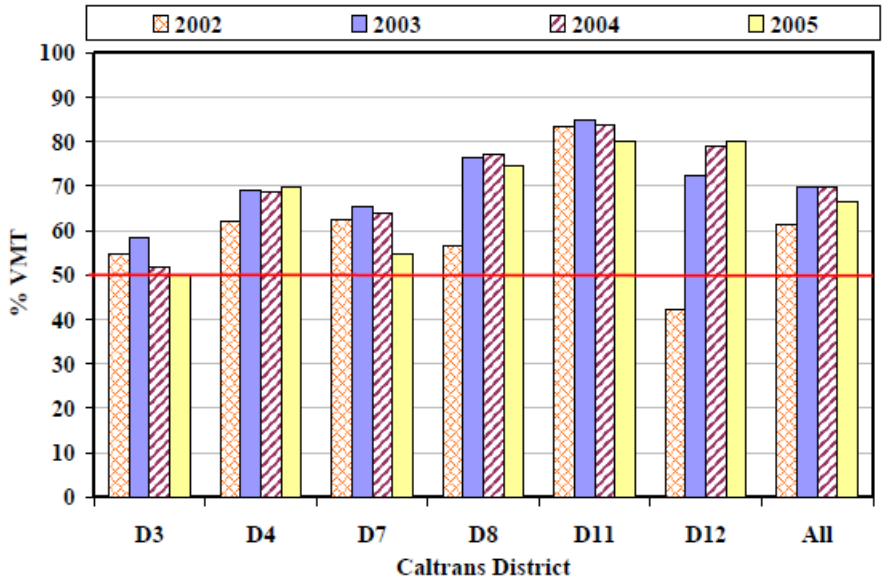

Figure 1-3.1 Percent of freeway VMT at speeds greater than 65 mph[7]

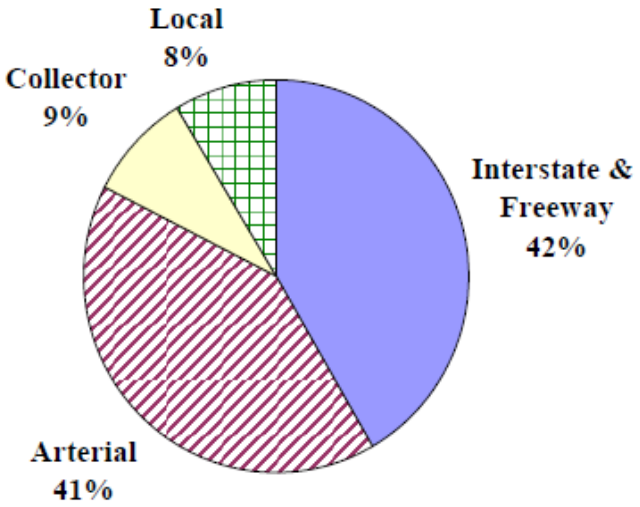

Figure 1-3.2 Percent of 2002 annual VMT by roadway functional class[7]

Figure 1-3.3 California map displaying Caltrans districts[8]

2. Testing Facility and Experimental Set-up

All tests were conducted at the University of California, Riverside Center for Environmental Research and Technology Light-Duty Chassis Dynamometer. This facility is a certification grade and has been operational since 1996. Furthermore, this facility has the capability to conduct light-duty gasoline, diesel and natural gas emissions testing up to 400 times a year using three different constant volume samplers, for each fuel type.

2.1 Vehicle Emissions Research Laboratory

The University of California, Riverside's (UCR) Center for Environmental Research & Technology (CE-CERT) is equipped with a state-of-the-art vehicle emissions research laboratory (VERL) for measuring light-duty vehicle exhaust emissions representative of real-world driving conditions. See Figure 2-2.1 this facility is equipped with a Burke E. Porter 48-inch light-duty chassis dynamometer capable of simulating dynamic driving cycles. This facility is capable of sampling exhaust from various vehicles and fuels. There are a three separate constant volume sampler (CVS) tunnels capable of providing diluted sample points for gasoline, diesel and natural gas exhaust. Multiple advanced particle measurement instruments are installed capable of continuous particle measurement. Furthermore, the lab is also equipped with analytical instruments for measuring regulated and unregulated gaseous emissions. Figure 2-2.1 shows the overall testing schematic.

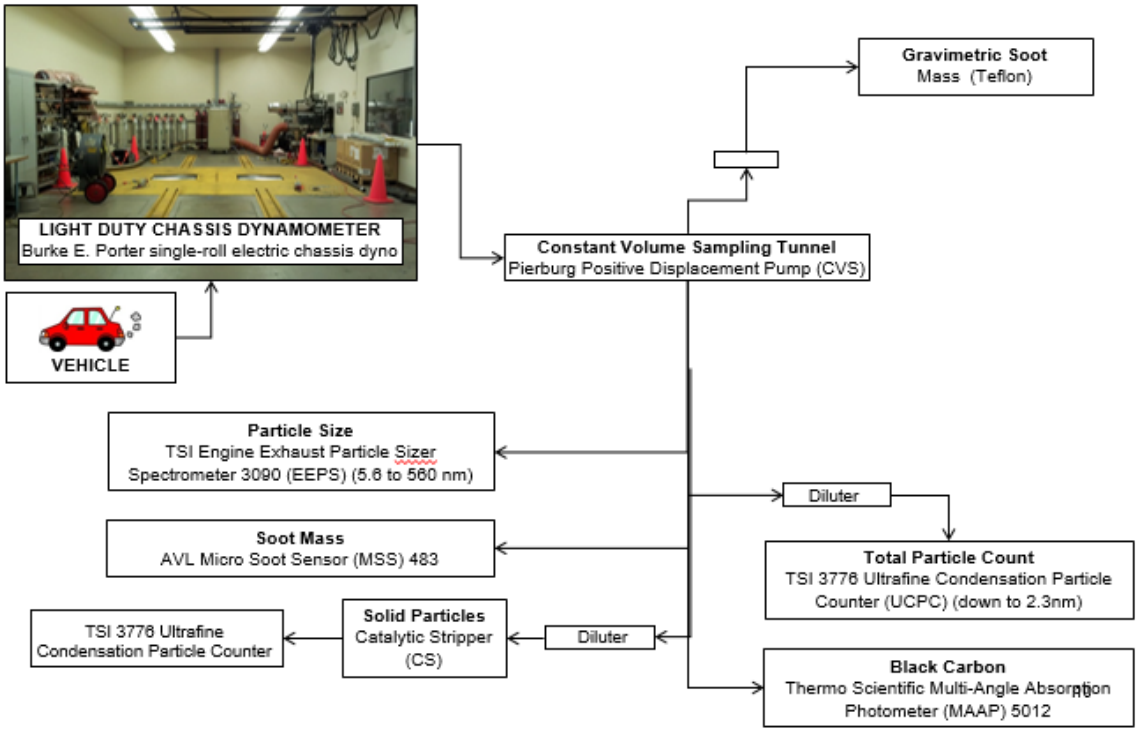

Figure 1-2.1 UCR's VERL set-up

2.2 Emissions Measurements

Particle phase emissions were measured for the entire driving cycle. Total particle count was measured using a TSI-3776 Ultrafine Condensation Particle Counter (UCPC). Solid particle number was measured using a catalytic stripper (CS). Particulate matter was measured with an AVL Micro soot sensor model 483, while black carbon (BC) was measured using a Thermo Scientific Multi-Angle Absorption Photometer (MAAP) model 5012 Particle size distributions were measured using a TSI-3090 Engine Exhaust Particle Sizer (EEPS). In this work we focus on particle number and composition. The instrumentation is described as follows.

2.3 Instruments

Total particle number was measured using a butanol based TSI-3776 UCPC. The working principle behind this unit consist of supersaturating aerosol with a vaporized working fluid, in this case butanol. The particle then grows due to the condensation of the working fluid vapor on the particle surface. The UCPC can optically detect particles after their growth[11]. For this study, an engine exhaust aerosol was continuously drawn from the constant volume sampler (CVS) and passed through a heated saturator area in which butanol is vaporized and diffused into the sample stream flow. Both the aerosol and the alcohol together pass through a cold condenser where the alcohol is super saturated and condenses onto the surface of the aerosol sample. The engine exhaust aerosol sample acts as condensation nuclei, and the aerosol particles grow in diameter into larger droplets and pass through an optical counter where the UCPC counts them[12]. A schematic of this process is shown in Figure 2-3.1.

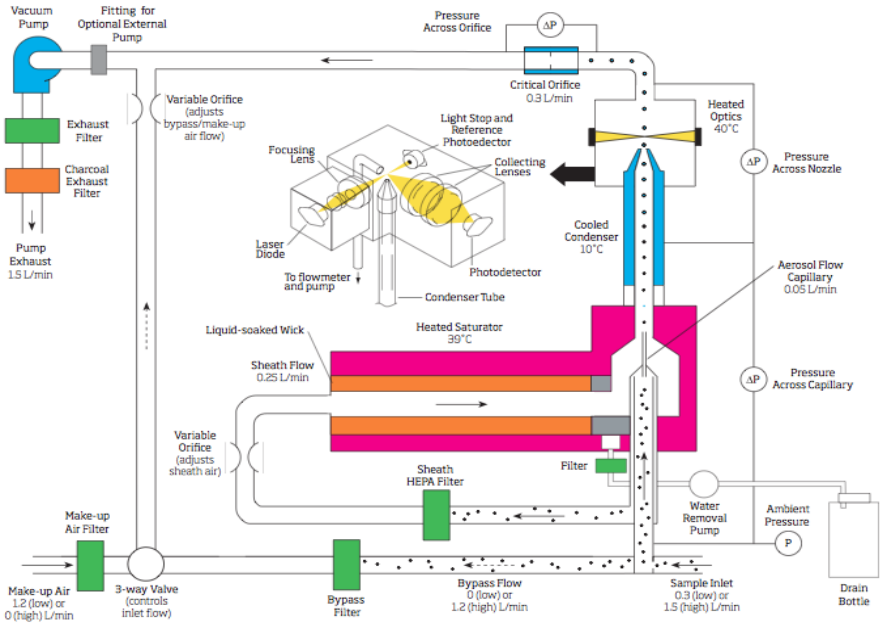

Figure 2-3.1 TSI UCPC 3776 operation diagram[17]

This unit counts aerosol particles and is capable of fast aerosol concentration change response. It can count up to 300,000 particles·cm^{-3} and is capable of detecting particles down to 2.3 nanometers in diameter.

In addition to total particle count, particle size distribution measurements were taken using TSI's EEPS model 3090. This unit is capable of continuous particle number concentration measurement from exhaust with a fast time resolution. It measures the size distribution and concentration of engine exhaust within a range of 5.6 to 560 nanometers[13]. The instrument draws sample exhaust from the CVS continuously. Sample particles are positively charged using a corona charger. Then, these newly charged particles are introduced to a region near the center of a high-voltage electrode column and transported downwards through filtered sheath air. A positive voltage is applied to the electrode and a repulsion force is created. This repels the positively charged particles outward according to their electrical mobility. Next, particles with a high electrical mobility strike electrometers near the top where particles with a low electrical mobility strike near the bottom[13]. This allows for simultaneous concentration measurements of multiple particle sizes. See Figure 2-3.2 for a flow schematic. Lastly, the EEPS transforms raw data into particle size and concentration using a real-time data inversion. This accounts for variability in particle charge.

Particulate matter and black carbon were both measured for this study using an AVL micro-soot sensor model 483 and a Thermo Scientific MAAP model 5012, respectively. The AVL micro-soot sensor measures varying soot concentrations with high sensitivity, having a detection limit of 5 μg·m^{-3}. The measuring principle is photo-acoustics. Sample diluted exhaust is pulled from the CVS and directed through a measuring chamber that is thermally

animated by a laser beam. The modulated heating produces periodic pressure pulsation, which is detected by a microphone as an acoustic wave[14]. This is depicted in Figure 2-3.3.

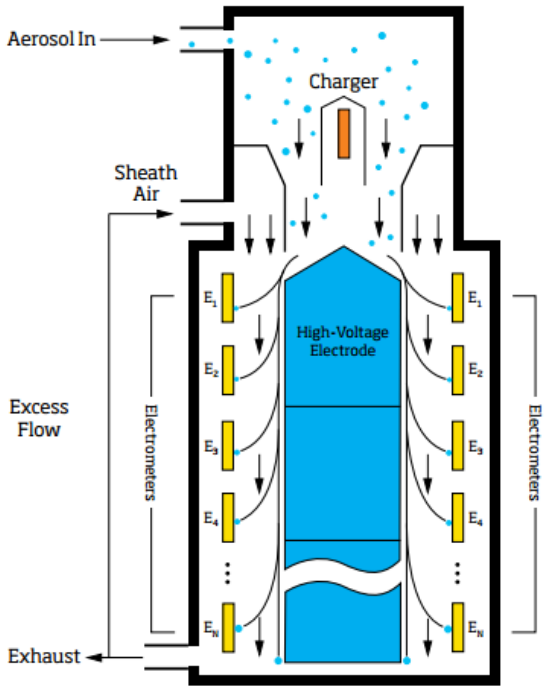

Figure 2-3.2 EEPS flow schematic[18]

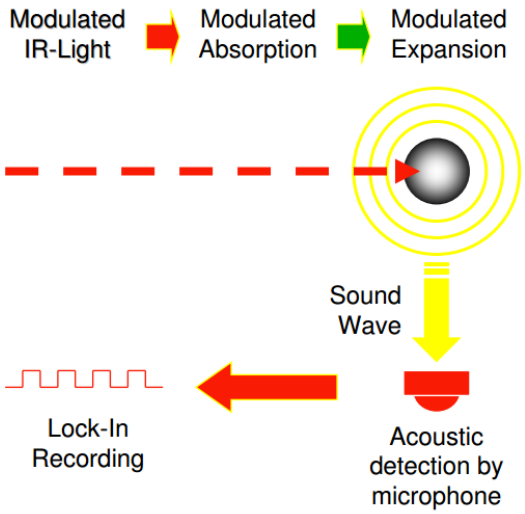

Figure 2-3.3 AVL MSS 483 Measuring Principle[19]

Thermo Scientific's MAAP model 5012 measures BC by optical means. This is done by using a radiative transfer scheme to particles loaded on glass fiber filters. Typically, BC measurements by optical means measure the transmission of light through the filter on which the BC was loaded. This posed inaccuracies due to the reflection and scattering of light in multiple directions caused by the shape and size of the BC particle. The MAAP during operation, however, contains multiple detectors simultaneously measuring transmitted and scattered light, thus potentially eliminating inaccuracies due to scattering.[15]. This measurement principle is shown in Figure 2-3.4.

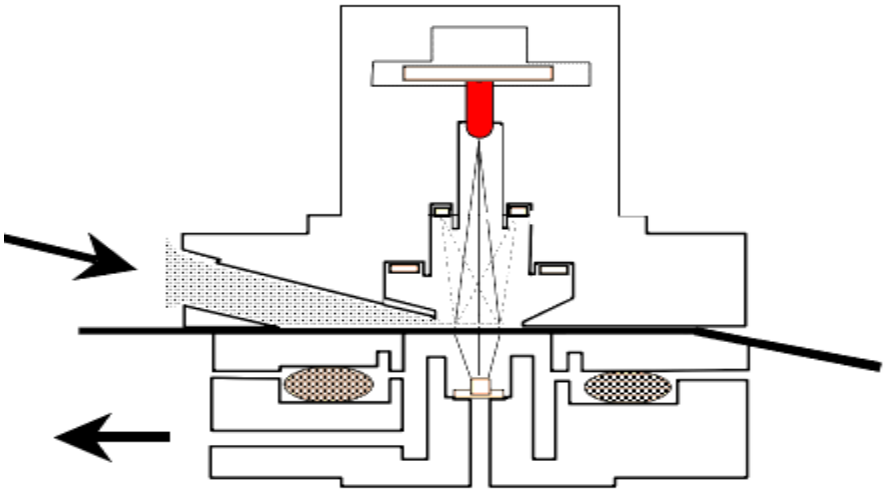

Figure 2-3.4 MAAP measurements include Transmittance and Reflectance of BC[20]

For this study, a catalytic stripper (CS) was also used to measure total solid particle number. This CS is consistent with the one used in Ntziachristos et al 2013. This consisted of a cordierite monolith with silica-alumina coating with a cell density of 400 cells per square inch and 2.5 mil wall thickness[16]. The CS also consists of a 26 mm long platinum-based catalyst and a sulfur trap consisting of barium oxide. The residence time has been documented to approximately a third of a second[16]. The temperature for this study

remained constant with theirs at 300ºC. The operating principle behind the CS is that organic species with the potential to nucleate are oxidized. The CS draws sample from the secondary dilution (12:1) which draws directly from the CVS. After passing through the CS, particles pass through a cooling coil and are counted by another UCPC TSI model 3776. This CS set up has been shown to perform practically identical to the Particle Measurement Programme (PMP)[16].

2.4 Test Vehicles

While a broader range of light-duty vehicles were selected and tested, this study focused on emissions from spark-ignition direct-injection (SI-DI) vehicles. These were selected using on their EMFAC classes and emission standards, see Table 2-4.1.

Table 2-4.1 Vehicle Classes in EMFAC

Vehicle Class	**Fuel Type**	**Code**	**Description**	**Weight Class (lbs)**	**Abbreviation**
1	Gas, Diesel, Electric	PC	Passenger Cars	All	LDA
2	Gas, Diesel, Electric	T1	Light-Duty Trucks	0-3750	LDT1
3	Gas, Diesel	T2	Light-Duty Trucks	3751-5750	LDT2
4	Gas, Diesel	T3	Medium-Duty Trucks	5751-8500	MDV
5	Gas, Diesel	T4	Light-Heavy-Duty	8501-10000	LHDT1
6	Gas, Diesel	T5	Light-Heavy-Duty	10001-14000	LHDT2
7	Gas, Diesel	T6	Medium-Heavy-Duty	14001-33000	MHDT
8	Gas, Diesel	T7	Heavy-Heavy-Duty	33001-60000	HHDT
9	Gas, Diesel	OB	Other Buses	All	OBUS
10	Diesel	UB	Urban Buses	All	UBUS
11	Gas	MC	Motorcycles	All	MCY
12	Gas, Diesel	SB	School Buses	All	SBUS

Vehicle classes 1 through 3 were the light-duty vehicles considered in this study. Two sets of emission standards have been defined by the Clean Air Act Amendments (CAAA). These include, Tier 1 standards and Tier 2 standards. These were phased-in progressively in the late 1900's and 2000's, respectively. The total number of vehicles tested is 13 and consist of a mixture of passenger cars (LDA), Light-Duty Trucks (LDT1) under a gross vehicle weight of 3,750 lbs, and Light-Duty Trucks (LDT2) with a gross vehicle weight between 3,751 and 5,750 lbs. Their selection process is based on their population in the state. For example, LDT1 will have fewer vehicles to be tested because this class has a lower population in the state in 2012 when compared to the LDA and LDT2 classes. Furthermore, relatively newer model year vehicles will be given higher priority as they account for a higher fraction of the entire state's vehicle population[17]. A matrix of the vehicles tested is shown in Table 2-4.2.

Table 2-4.2 Vehicle Specifications

Vehicle Make and Model	**Class**	**Engine**	**Model Year**
Hyundai Accent	LDA	1.6L I4 GDI	2013
Nissan Versa	LDA	1.8L I4 PFI	2013
Volkswagen GLI	LDA	2.0L I4 T-GDI	2013
Toyota Rav4	LDA	2.0L I4 PFI	2003
Honda Accord	LDA	2.3L I4 PFI	2001
Kia Optima	LDA	2.4L I4 GDI	2013
Chevy Equinox	LDT2	2.4L I4 GDI	2014
Ford Escape	LDT1	2.5L I4 PFI	2013
BMW X5 xDrive 35d	LDT2	3.0L V6 DDI	2013

Chevy Impala	LDA	3.6L V6 GDI	2013
Mercedes-Benz E350 Coupe	LDA	3.6L V6 SP-GDI	2013
Toyota 4Runner	LDT2	4.0L V6 PFI	2014
Dodge Ram 1500	LDT2	5.9 V8 PFI	2002

Table 2-4.2 includes gasoline direct-injection (GDI), port-fuel-injection (PFI), spray-guided gasoline direct-injection (SP-GDI), turbo-charged gasoline direct-injection (T-GDI) and diesel direct-injection (DDI) vehicles.

2.5 Driving Cycles

In the 1990's, Caltrans along with CARB established the Caltrans/ARB Modeling Program (CAMP) in an effort to improve mobile source emissions inventory modeling in California. The program focused on improving speed correction factors associated with modeling emissions from various roadways. The CAMP project aimed to develop major breakthroughs in emissions modeling[9]. Some of the key ones include develop sampling methods to collect and record representative freeway driving conditions as well as develop adequate driving cycles and measure tailpipe emissions with a chassis dynamometer. This multi-year research project concluded with a large data set of driving and tailpipe emissions specific to California.

In CAMP, several driving cycles were developed using field driving data. For this study, the freeway driving cycles developed are in focus as high speeds are more likely to occur on freeways. These cycle developments concluded in two types of freeway driving cycles

using field driving data collected on Los Angeles freeways. LOS is based on traffic measurements taken by the Freeway Performance Measurement System (PeMS).

The LOS driving cycles represent various traffic congestion scenarios. This ranges from A (least congested) to F (most congested). The table below shows a distribution of the data used to develop the driving cycle. LOS A through D shows high spends, up to 68 mph, where LOS F shows a relatively slower speed, almost 32 mph.

Table 2-5.1 Los Angeles freeway driving data by LOS distribution[10]

LOS	No. of Seconds	Frequency (%)	Lock-On Rate (%)	Vehicle Speed (mph)		
				Min	Max	Mean
A	21,257	12.60	85.57	48.2	89.7	68.1
B	20,383	12.10	89.44	0	91.7	66.7
C	24,800	14.70	88.62	4.3	91.7	66.4
D	54,245	32.10	91.76	0	89.7	63.7
E	26,631	15.80	93.66	0	81.9	55.4
F	21,477	12.70	95.47	0	74.4	31.9
All	*168,793*	*100.00*	*91.01*	*0*	*91.7*	*59.7*

Table 2-5.2 Freeway driving cycles developed for the CAMP program[10]

Driving Cycle	Time (minutes)	Distance (miles)	Vehicle Speed (mph)			Time at Speed >= 65 mph	
			Min	Max	Mean	Seconds	%
LOSA	6.65	7.51	55.6	79.5	67.8	287	71.9%
LOSAT	9.42	10.68	53.7	81.6	68.1	388	68.7%
LOSB	6.10	6.80	51.7	78.3	66.9	234	63.9%
LOSC	7.47	8.28	47.8	78.7	66.5	312	69.6%
LOSD	7.22	7.85	48.2	77.6	65.3	224	51.7%
LOSDT	9.00	9.67	40.6	75.3	64.5	277	51.3%
LOSE	7.85	7.49	16.1	74.4	57.2	135	28.7%
LOSET	9.02	8.64	26.5	77.0	57.5	120	22.2%
LOSF	8.93	4.85	3.9	63.9	32.6	0	0.0%
S1020	**7.43**	**1.88**	**0**	**65.4**	**15.2**	**1**	**0.2%**
S2030	**3.25**	**1.38**	**11.0**	**40.0**	**25.4**	**0**	**0.0%**

S3040	**7.78**	**4.25**	**5.1**	**53.7**	**32.8**	**0**	**0.0%**
S4050	**6.63**	**5.05**	**28.6**	**63.1**	**45.7**	**0**	**0.0%**
S5060	**8.63**	**8.14**	**36.0**	**65.4**	**56.6**	**17**	**3.3%**
S6070	**8.38**	**9.12**	**56.0**	**73.3**	**65.3**	**276**	**54.9%**
S7080	**8.60**	**10.45**	**66.6**	**82.3**	**72.9**	**516**	**100.0%**

Table 2-5.2 above summarizes the driving cycle characteristics developed for the CAMP program. The column labeled as driving cycle represents the name of the driving cycle developed. Moving across the table several characteristics are shown, including vehicle speed in a minimum, maximum and mean value as well as the time this cycle spends at a speed higher than or equal to 65 mph displayed as a percentage. The table shows that cycle LOS A has the highest mean speed among the LOS group. LOS A has a mean speed of 67.8 mph for which 72% of the time the cycle accounts for a speed of 65 mph or greater.

In this study, a total of 8 different driving cycles were selected. From Table 2-5.2, S1020, S2030, S3040, S4050, S5060, S6070, S7080 were selected. The figures below represent a speed trace with mph on the y-axis and time in seconds on the x-axis. Another cycle, cycle DSID158 was also chosen as this cycle has a mean speed of 76 mph while 100% of the time the speed is above 65 mph. This cycle was developed by the U.S. Environmental Protection Agency's Motor Vehicle Emission Simulator (MOVES).

Both driving cycles S7080 and DSID158 have been chosen due to the characteristics of their speed and duration. The cycles become the type of high speed driving on freeways that is of interest for this study.

Table 2-5.3 Driving cycles used in this study

	Cycle 1		*Cycle 2*	
Speed	**Low**	**High**	**Low**	**High**
Camp Cycle Phases	S1020, S2030	S7080, DSID158	S3040, S4050	S5060, S6070

Table 2-5.3 shows two different speed phases per cycle used for this study. Cycle 1 low speed consists of CAMP speed cycles S1020 and S2030, while Cycle 1 high speed consists of CAMP speed cycle S7080 and MOVES speed cycle DSID158. Cycle 2 low speed consist of CAMP speed cycles S3040 while Cycle 2 high speed consists of CAMP speed cycle S5060 and S6070. The figures below represent a speed trace of the driving cycles, specific to low and high speed. These also show a transient nature for both cycles. While cycle 1 exhibits a more dramatic difference between low and high speed than cycle 2.

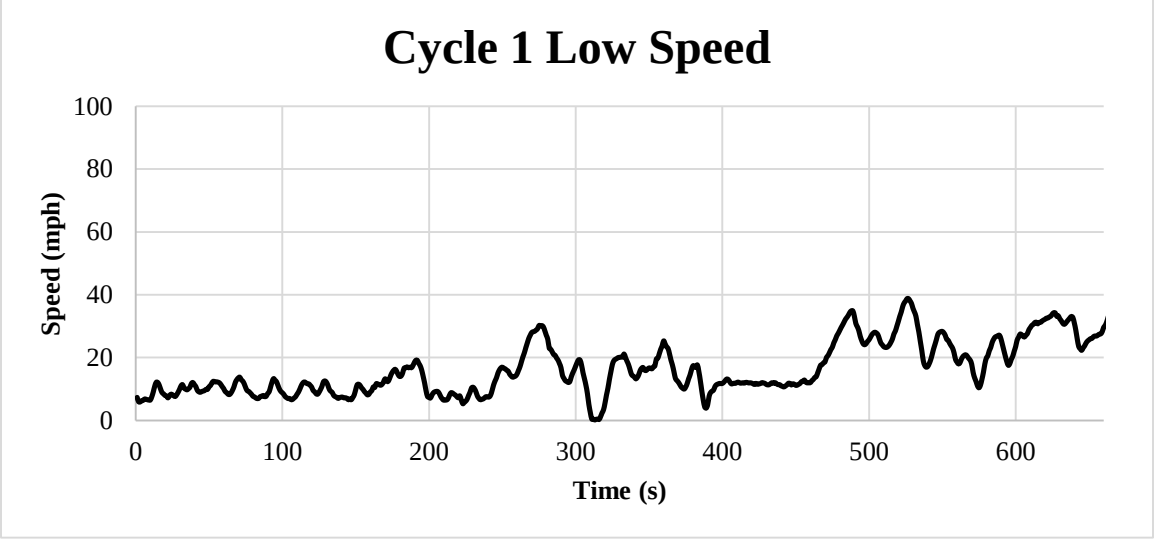

Figure 2-5.1 Cycle 1 Low Speed Trace

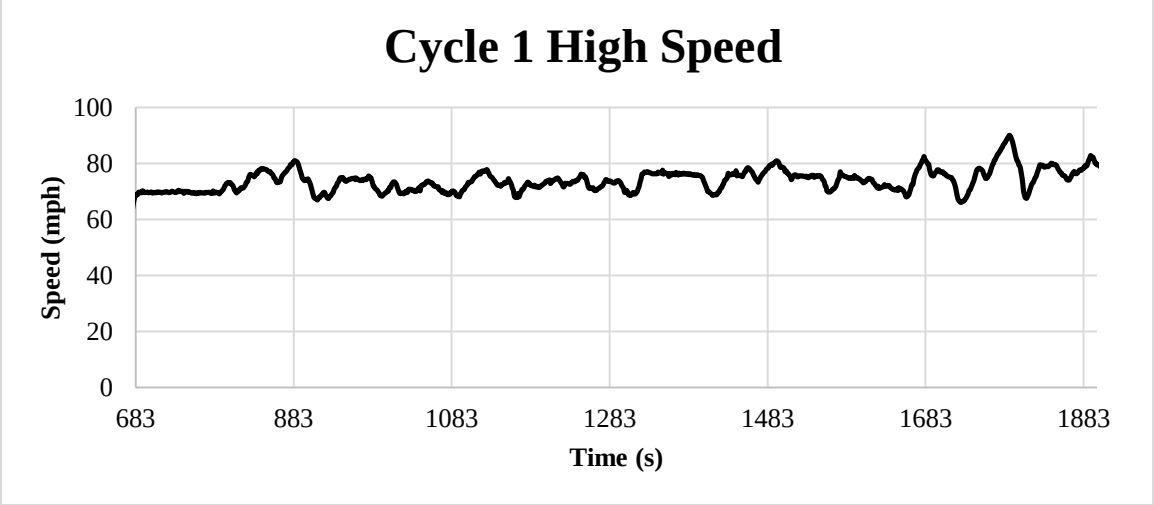

Figure 2-5.2 Cycle 1 High Speed Trace

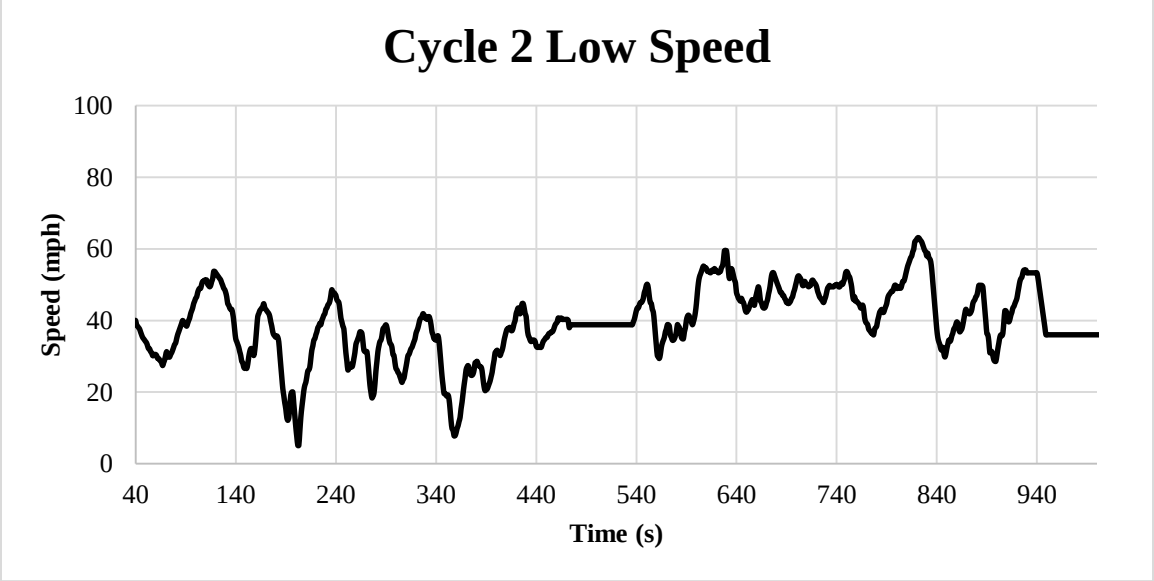

Figure 1-4.3 Cycle 2 Low Speed Trace

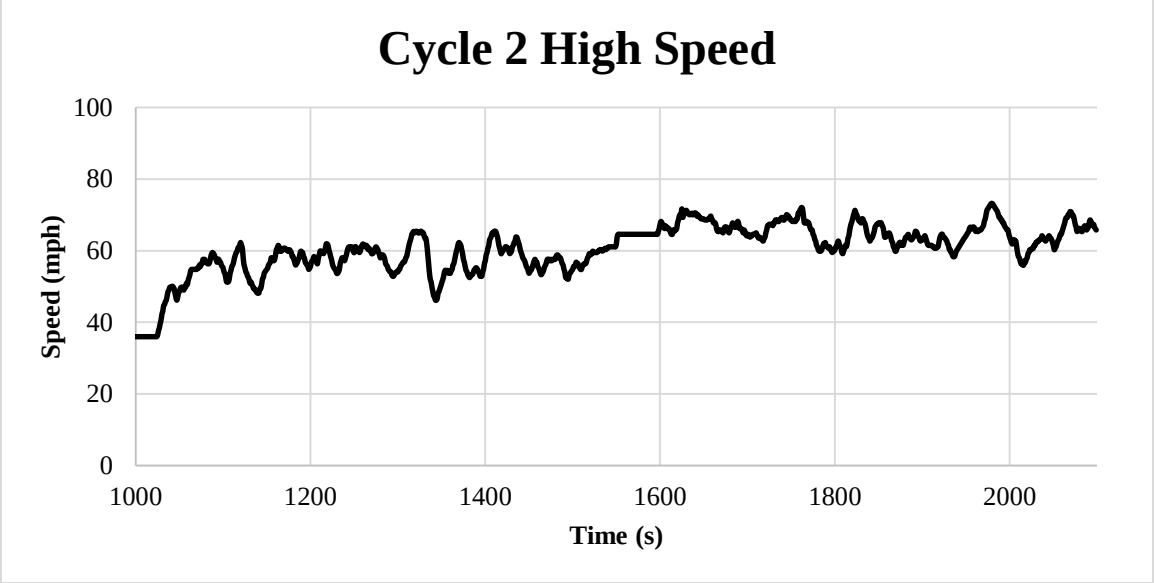

Figure 1-4.4 Cycle 2 High Speed Trace

3. Results and Discussion

The results are presented by first examining the effects of low versus high speed driving and their impacts on particle emissions from a fleet of GDI and PFI vehicles. The results are presented over a range of different measurements which can be affected by the amount of volatile and non-volatile composition of aerosol.

3.1 Total Particle Number

Total particle number was measured and reported in this study in units of particle number per mile. The average particle number concentration for low and high speed driving measured from the CVS, was multiplied by a dilution factor of 12:1 and by the total volume of air through the CVS corrected for standard temperature and pressure during each cycle

phase. This resulted in the total particle count for low and high speed. From this, the total particle count per phase was divided by the total miles traveled, giving the overall total particles per mile. A summary of the total particle number per mile for the fleet as a function of speed for cycle 1 and 2 is given in the figure 3-1.1 and figure 3-1.2. The figures above shows that for 77% of the vehicles, both GDI and PFI technology produced higher particle count during high speeds.. Furthermore, a more dramatic effect can be seen if we compare the low speed and the high speed emissions for cycle 1 than for cycle 2, this can be attributed to the nature of the cycle. Cycle 1 has a larger difference between the low and high speed. The average speed for the low phase of cycle 1 is 25 mph while the average speed for the high speed phase is 75 mph, that's a 50 mph difference. In cycle 2 however, the low speed average is 55 mph while the high speed average is 75 mph, that's a 20 mph difference.

If we compare total particle count between a GDI and PFI vehicle as a function of speed we can see that PFI vehicles emit higher total particle number than GDI. For the slow speed, PFI vehicles emitted an average of $1x10^7$ total particles per mile compared to $9x10^6$ particles per mile for the GDI vehicles. However during high speed, PFI vehicles emitted $2.6x10^7$ particles per mile while the GDI emitted $1.3x10^7$ particles per mile. That is a 21% and 52% difference between vehicles for low and high speeds respectively, See figure 3-1.3. Previous studies have shown that particle number emissions from gasoline engines tend to increase significantly when operated under high-load and transient conditions, this is because engines under high speed operate in fuel rich ratios, this is to maximize torque and reduce knock[10]. Furthermore, PM emissions from PFI engines have been shown to be

quite unstable[10]. Studies have found that PFI vehicles can have random spikes in PM emissions and these spikes were found to be volatile particles of less than 30nm in diameter[10].

Previous studies using a chassis dynamometer test have reported an average concentration of x 10^8 particles/cm^3 for older PFI vehicles. In contrast, similar studies conducted by the same authors found that a modern PFI vehicle can emit an average particulate number concentration ranging from 10^5 particles/cm^3 at light load to 10^7 particles/cm^3 at high load[11]. Particles released during these spikes were measured to be nearly all volatile less than 30nm in diameter. It is believed that these particles are formed through the nucleation of hydrocarbons released during combustion chamber deposit breakup[11]. A similar phenomenon may have occurred during this study as measurements show the older PFI vehicles exhibit high particle number count during high speed driving. The spikes can be seen in the real-time data plot in figure 3-1.4, where the PFI engine is in blue and the GDI engine is in red. Furthermore, correlations between total particle number and PM mass show a higher correlation than solid particle number and PM mass, suggesting that the spikes may contain volatile particles.

A diesel vehicle was also tested and it resulted in particle emissions that are below both the PFI and GDI engines. The diesel vehicle emitted an average of 1.4 x 10^6 particles/cm^3 during the low speed phase of cycle 1 and 2, and an average of 3.0 x 10^6 particles/cm^3 during the high speed phase of cycle 1 and two. A bar graph is shown in figure 3-1.5, comparing the average GDI, PFI and Diesel particle densities in red, blue and gold respectively. The diesel vehicle was equipped with a diesel particulate filter and thus is

expected to have lower particle densities than its gasoline counterparts. Furthermore, a real-time plot is shown in figure 3-1.6 which displays the diesel vehicle having the lowest count between the PFI and GDI vehicles.

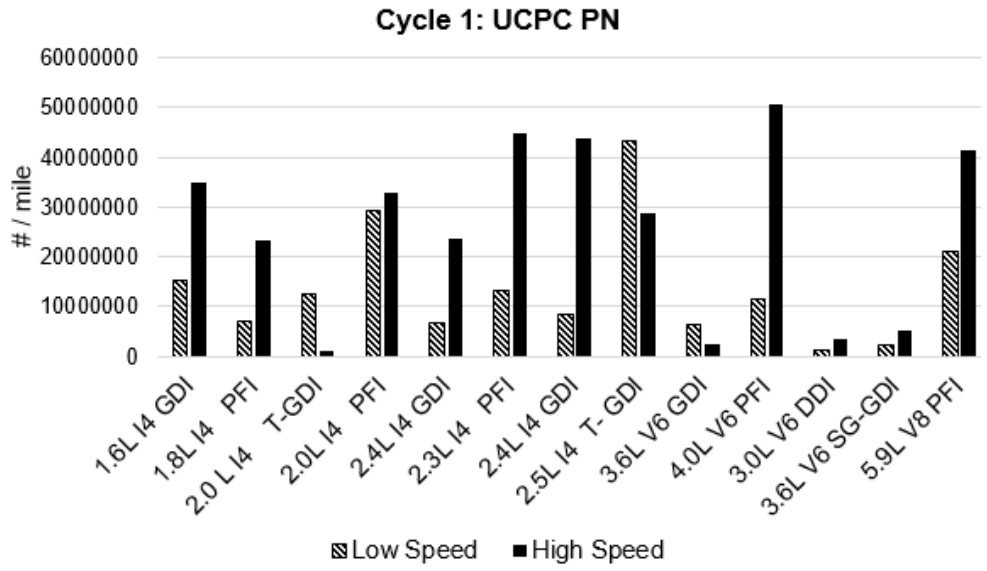

Figure 3-1.1 Total particle number per mile for low and high speed cycle 1

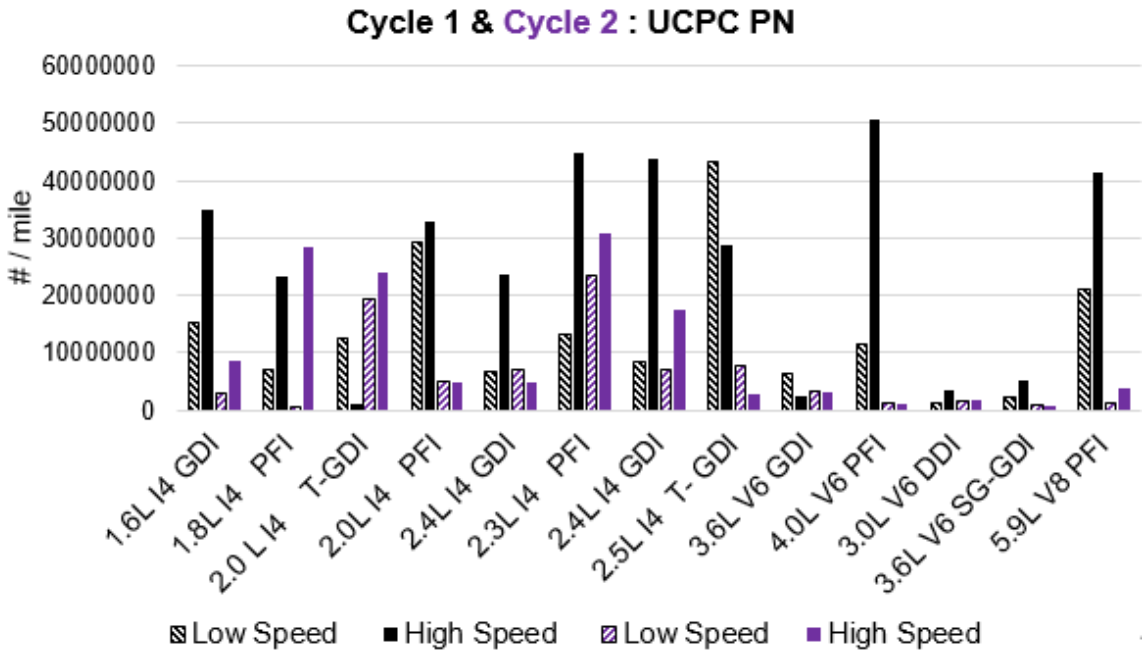

Figure 3-1.2 Total particle number per mile for low and high speed cycle 1 and 2

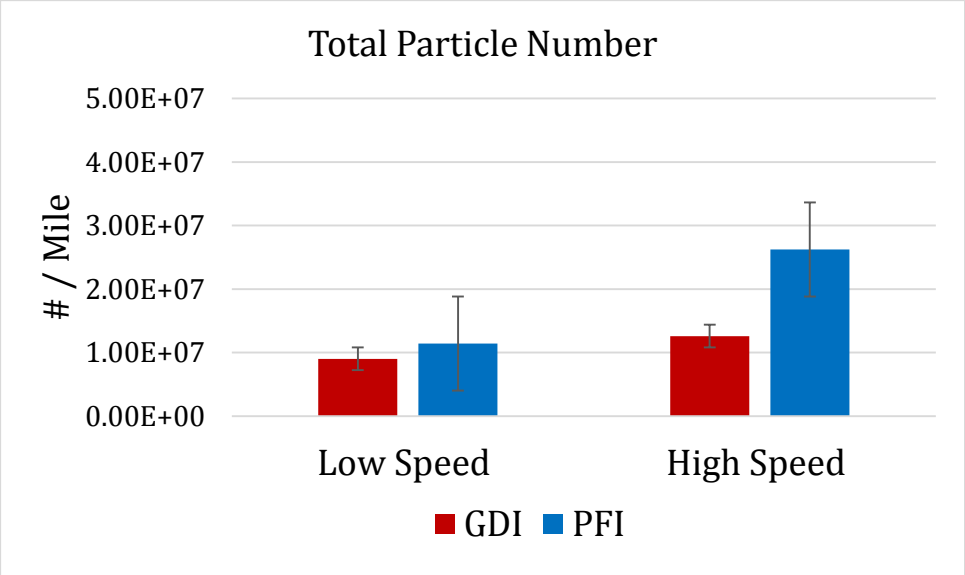

Figure 3-1.3 Total particle number count comparison for GDI and PFI vehicles

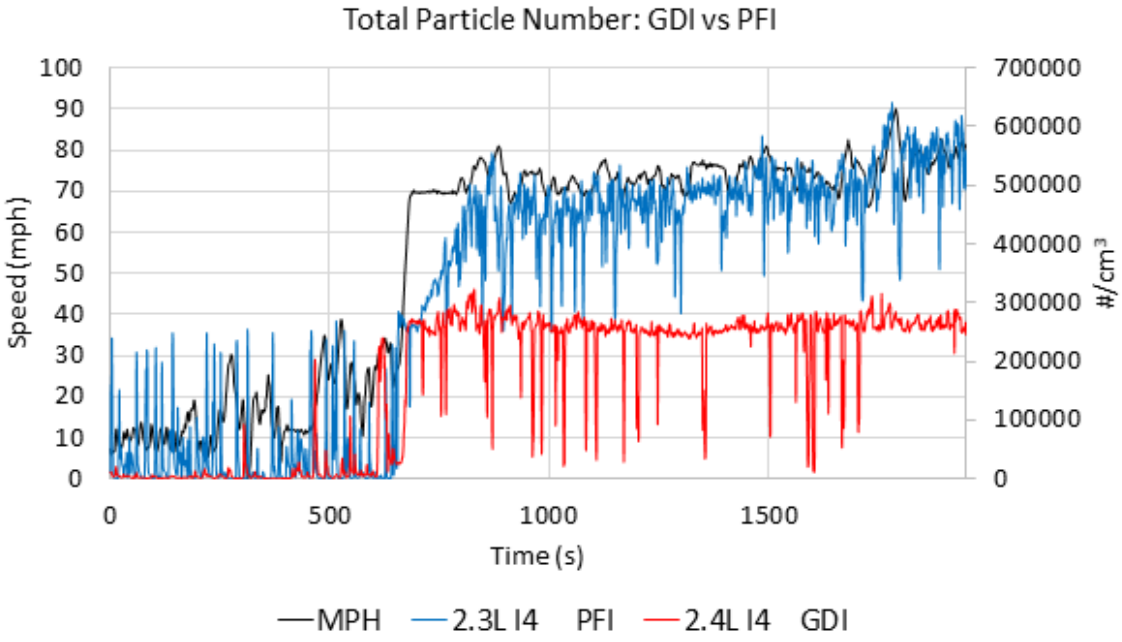

Figure 3-1.4 Total particle number real-time cycle 1 plot

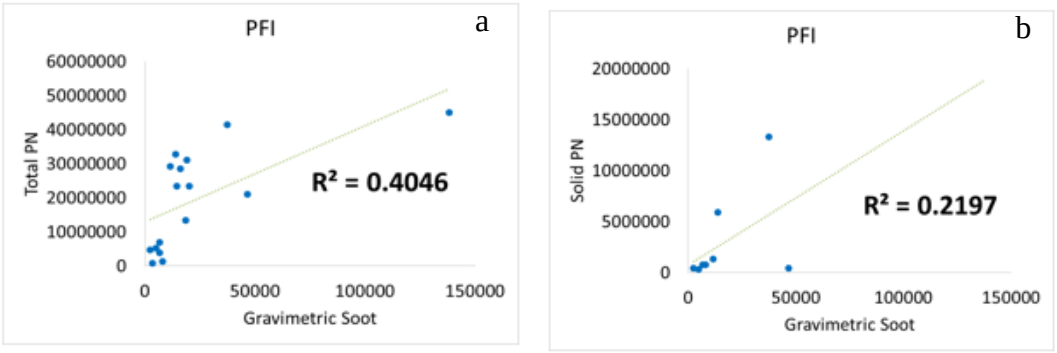

Figure 3-1.4a,b. a, total particle number (PN) correlated with PM mass and b, solid particle number correlated with PM mass.

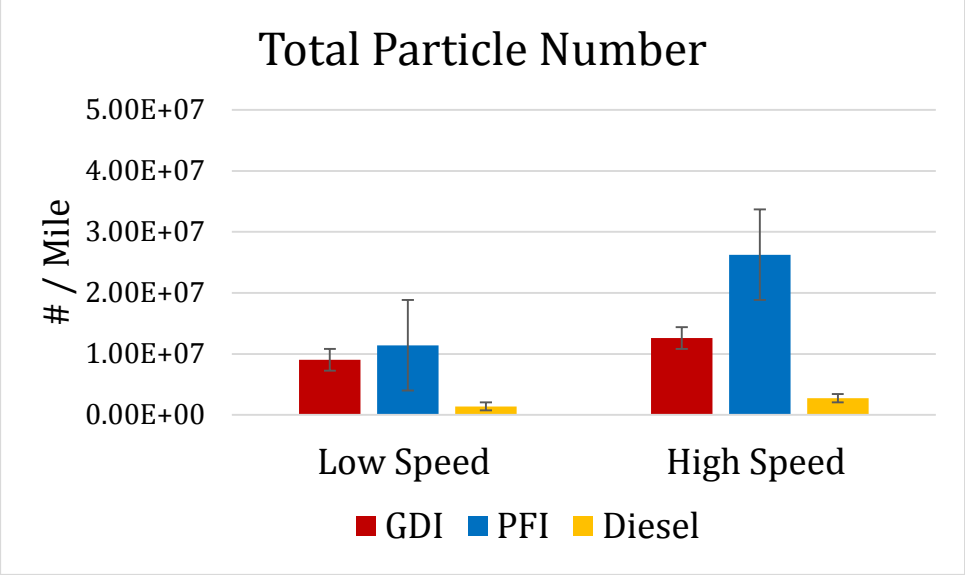

Figure 3-1.5 Total particle number for the GDI and PFI fleet and one diesel vehicle

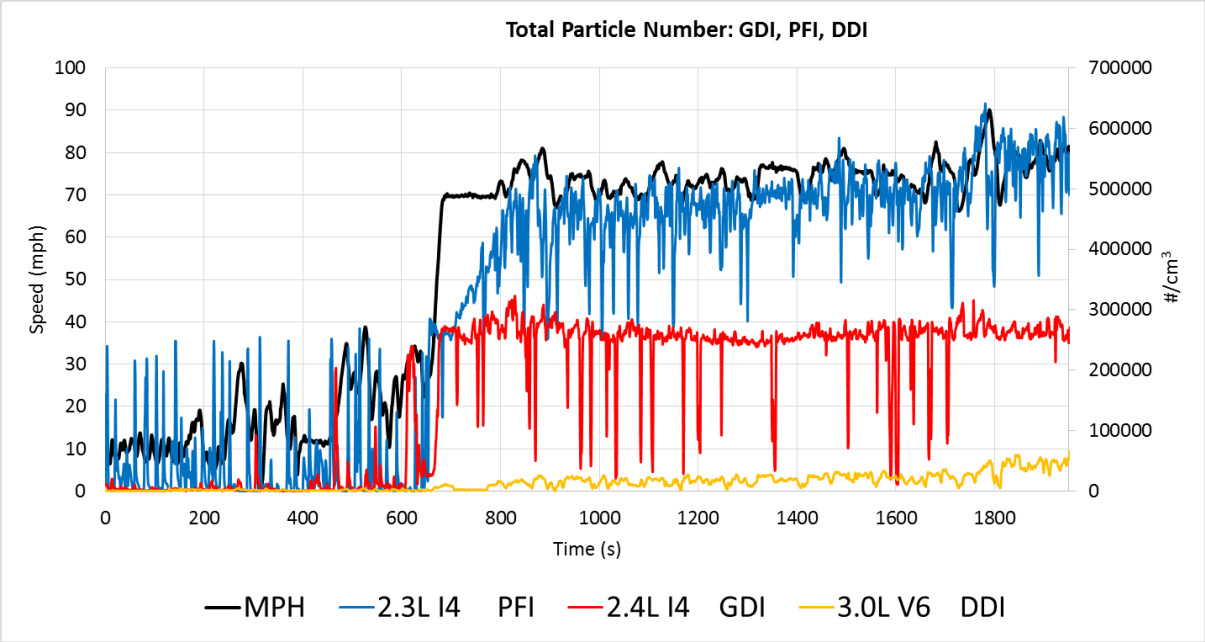

Figure 3-1.6 Total particle number for a GDI, PFI, and diesel vehicles

3.2 Solid Particle Number

Solid particle number important for regulations. Unlike the United States, Europe began regulating solid particle number from light duty passenger vehicles for spark-ignition direct-injection vehicles in 2012. The definition of solid is in analogy to that of PM. Solid particles are defined in European regulations as an operational one. That is to say that the definition is based on conventions and limitations imposed by the sampling protocol. Solid particles are particles which are counted with a particle number counter that has a 50% counting efficiency at 23nm at a temperature of 300 degrees Celsius. The catalytic stripper system was added to several weeks after the testing campaign had started, and thus not all vehicles were measured. This study found that for both GDI and PFI vehicles, solid particle number increased with increasing speed, this can be seen by comparing the

black bar to the stripped bar in figure 3-1.1. A study conducted using this system also concluded that emission levels depend on the driving cycle and high speed correlates well with an increase in solid particle number[16]. Again this difference may not be seen during cycle 2 due to the lower difference between low and high speed driving. When directly comparing the GDI to PFI fleet, GDI shows a higher solid particle count than the PFI. This trend is expected as GDI tend to produce higher soot than conventional PFI vehicles[16]. See figure 3-2.3. A real-time plot of solid particle emissions can be seen in figure 3-2.4, which indicates that the GDI vehicle is substantially higher than the PFI vehicle. Furthermore, it is important to note that the diesel vehicle was substantially lower than both the GDI and PFI.

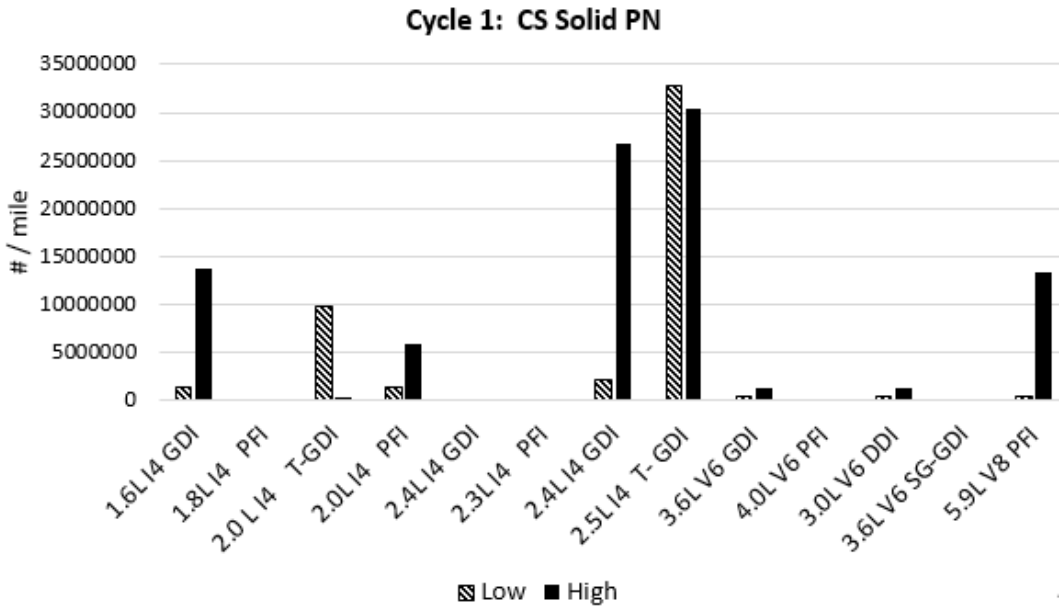

Figure 3-2.1 Solid particles per mile for cycle 1 as a function of low and high speed

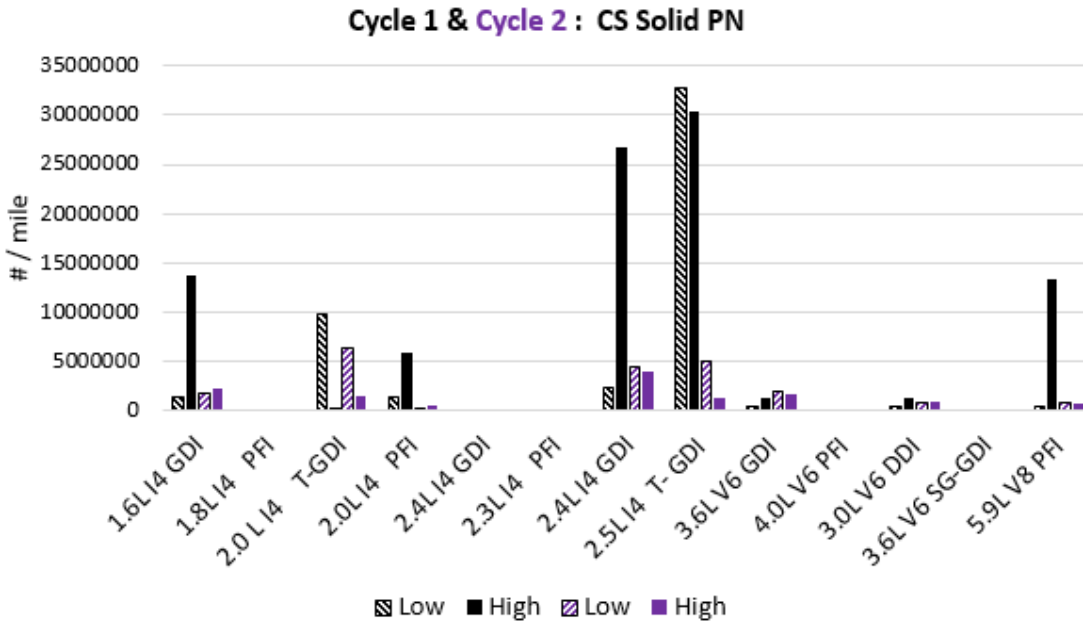

Figure 3-2.2 Solid particles per mile for cycle 1 and 2 as a function of low and high speed

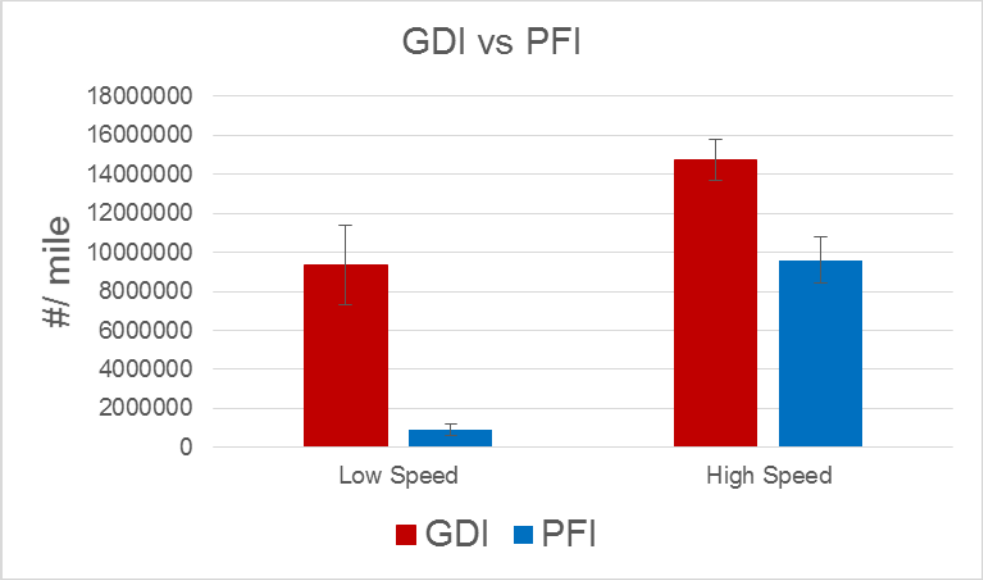

Figure 3-2.3 GDI and PFI solid particle comparison

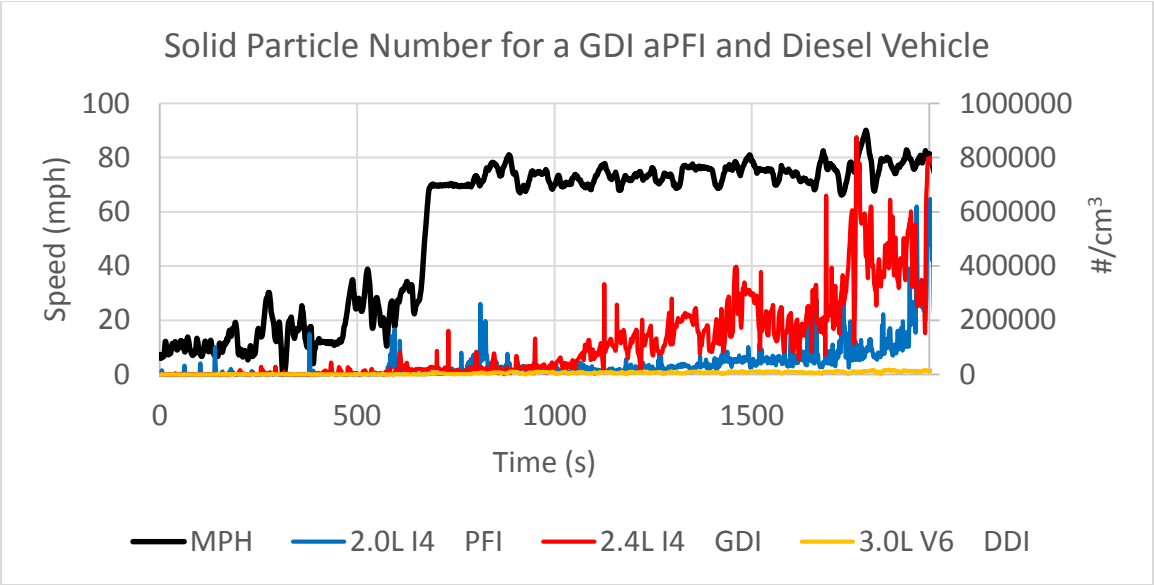

Figure 3-2.4 Real-time solid particle count for a GDI and PFI vehicle

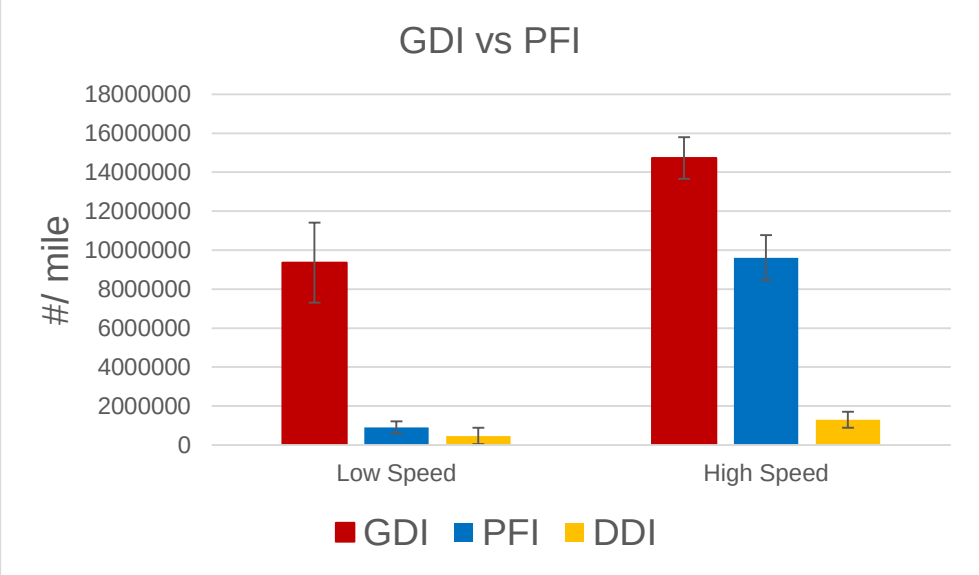

Figure 3-2.5 Solid particle count for a GDI, PFI and Diesel vehicle

3.4 Black Carbon and Soot Mass

Black carbon and soot particles are important for climate change effects. Black carbon can have a warming effect that rivals that of methane gas. For this study, black carbon and soot were measured using the photometry and photo-acoustic principles. A bar graph displaying black carbon concentrations per mile is shown as functions of speed in figure 3-4.1. This displays that low speed driving exhibits higher black carbon concentration than high speed driving. This is also apparent during cycle 2. The measurement technique involves shining a 670 nm light through the filter paper to observe its reflectance. At this wavelength, it is possible to measure brown carbon (BrC) which has been shown to absorb wavelengths in the range of 440-870 nm[23]. It may be possible that the high black carbon readings consistently during cycle 1 and 2 may be due to BrC. Photo-acoustic measurements showed a different trend. Higher speed driving exhibited higher concentrations of soot than lower speeds. This can be seen in figure 3-4.3. For cycle 2, the data is closer together and thus the trend is not shown. PM mass measured through collecting material on a Teflon filter shows a similar trend to the photo-acoustic soot. Higher speed driving exhibits higher soot concentrations, however the difference between high and low speed soot is not as dramatic as either the black carbon measurements or the photo acoustic soot measurements. This can be due to the measurement technique, in which Teflon filters can have organic material which would not be measured with the other instruments. It is important to note that when comparing GDI to PFI vehicles, GDI

vehicles exhibited higher concentrations of black carbon and soot for low and high speed driving. The PM mass however displayed the PFI vehicles to have more soot than the GDI vehicles, again this can be accounted by the organic material present in Teflon filters. See figures 3-4.7 through 3-4.9.

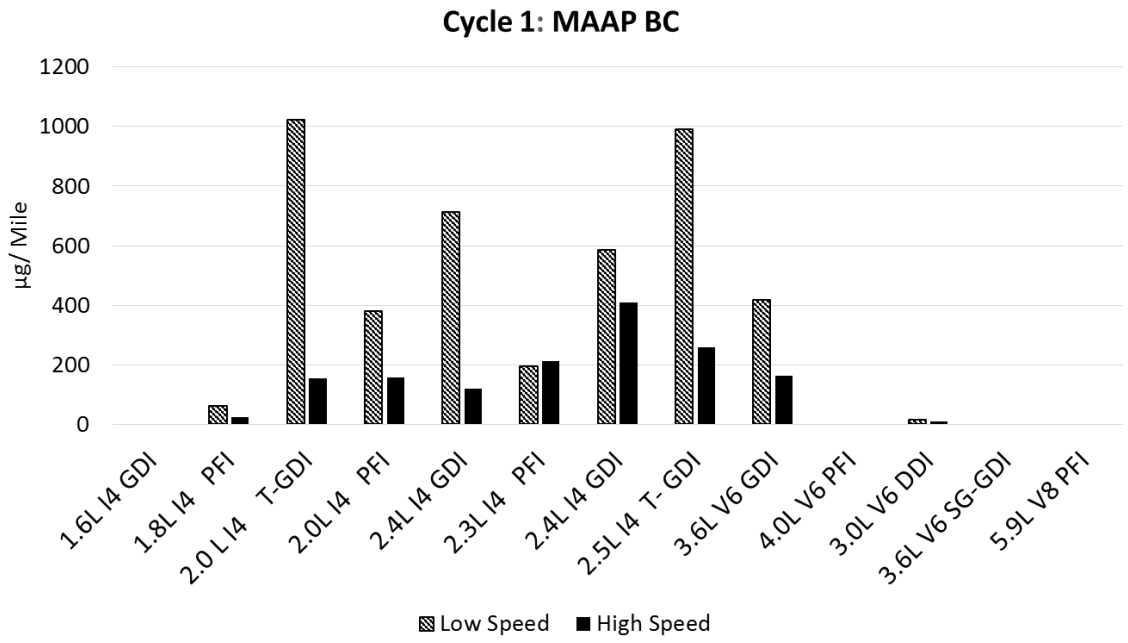

Figure 3-4.1 Black carbon measurements across the fleet during cycle 1

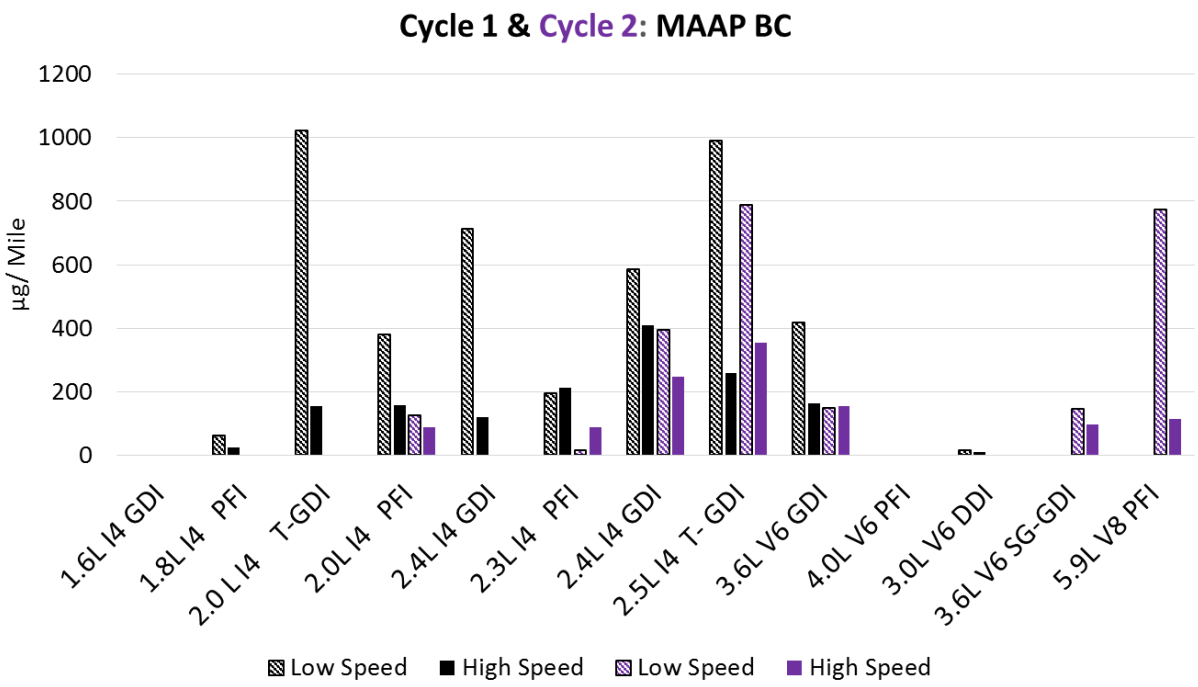

Figure 3-4.2 Black carbon measurements across the fleet during cycle 1 and 2

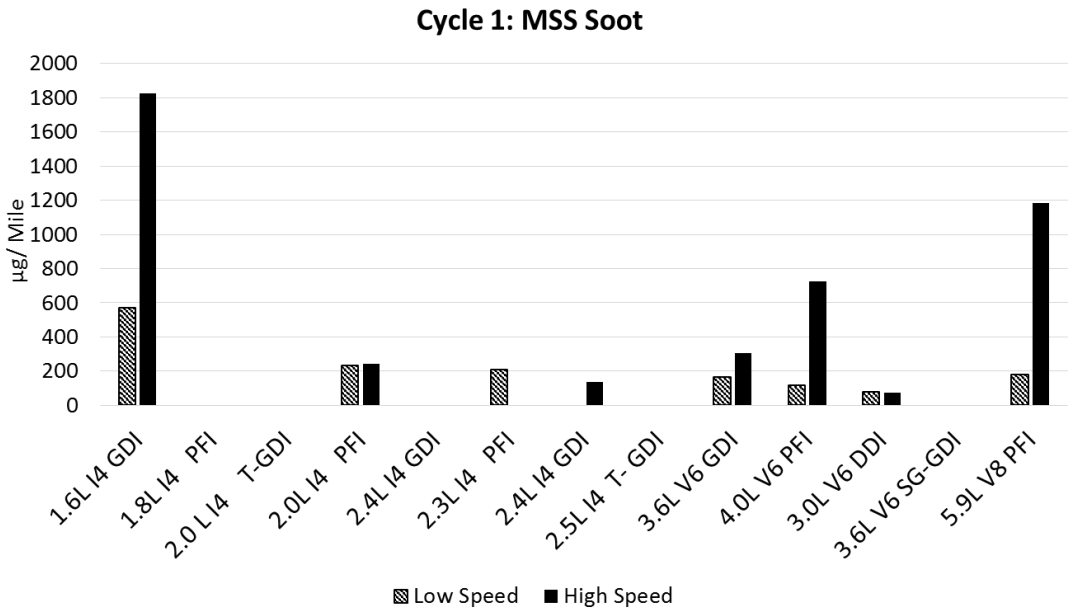

Figure 3-4.3 Soot measurements across the fleet during cycle 1

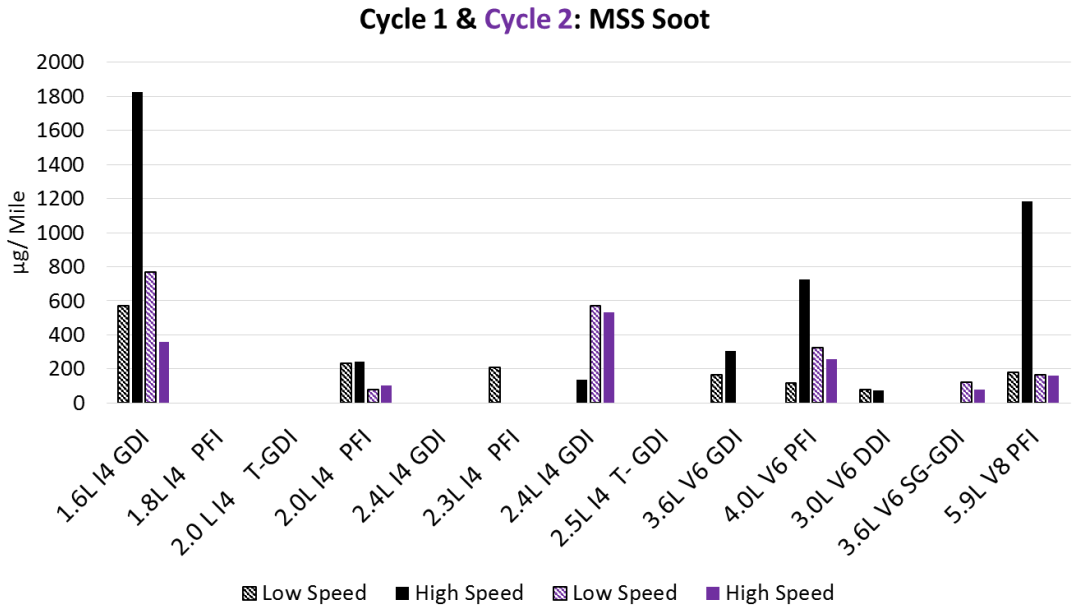

Figure 3-4.4 Soot measurements across the fleet during cycle 1 and 2

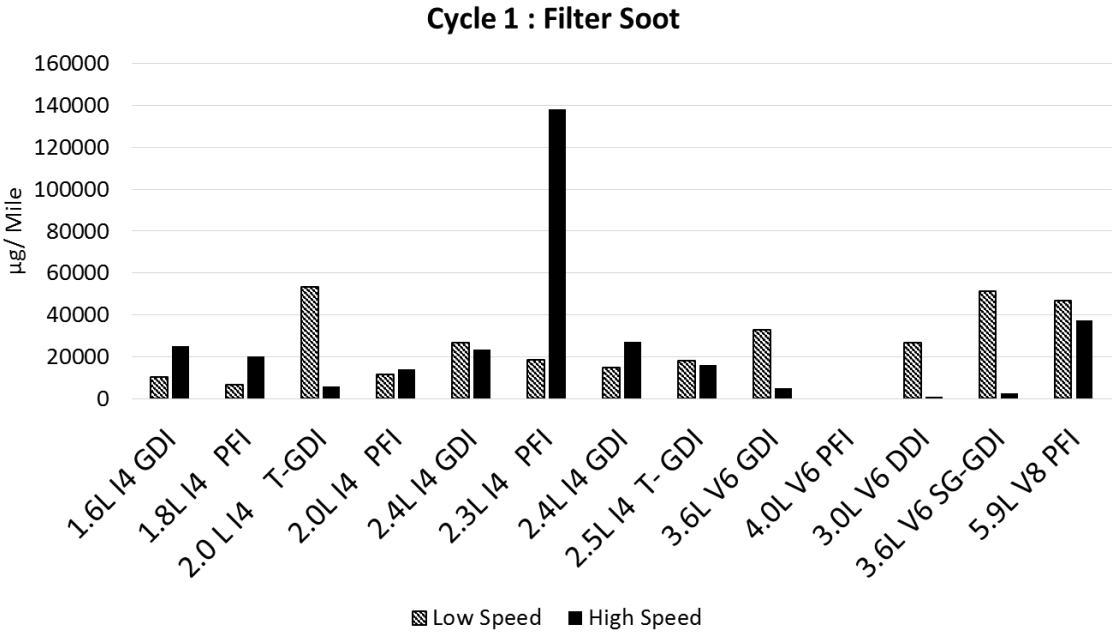

Figure 3-4.5 Filter soot measurements across the fleet during cycle 1

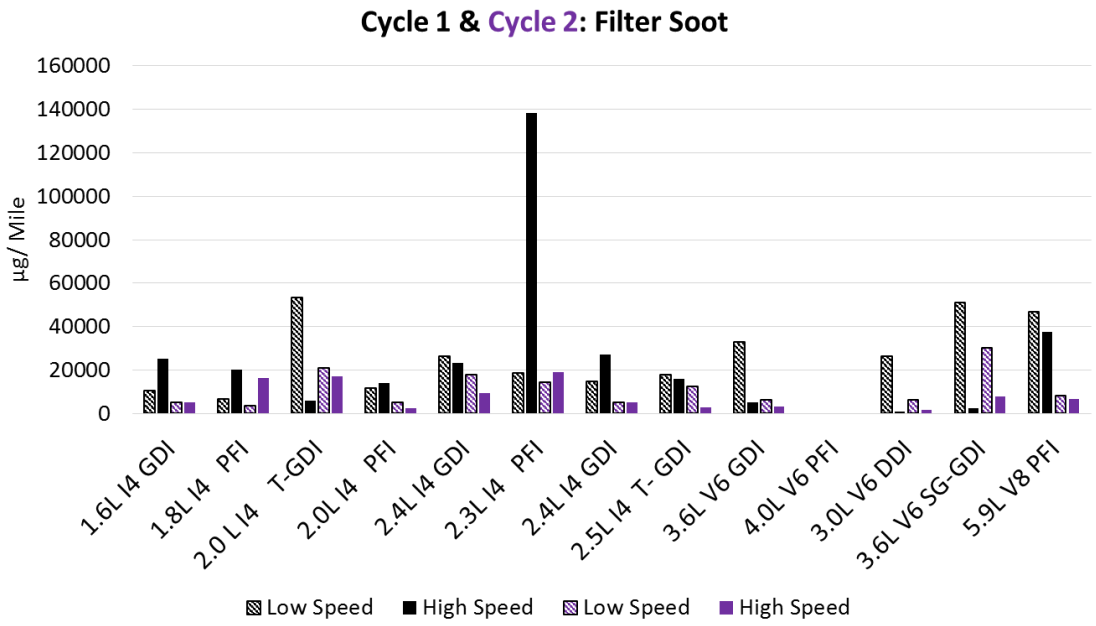

Figure 3-4.6 Filter soot measurements across the fleet during cycle 1 and 2

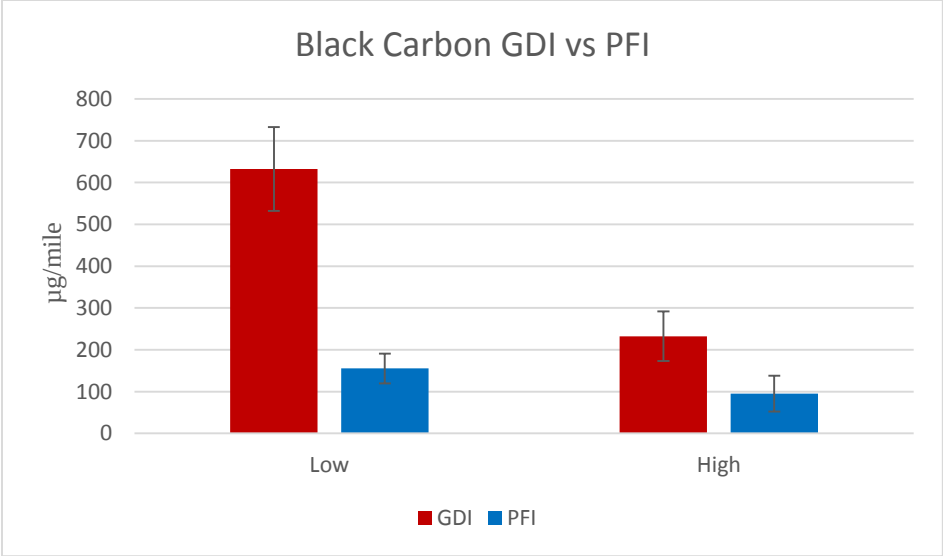

Figure 3-4.7 Black carbon comparison between a GDI and PFI vehicle

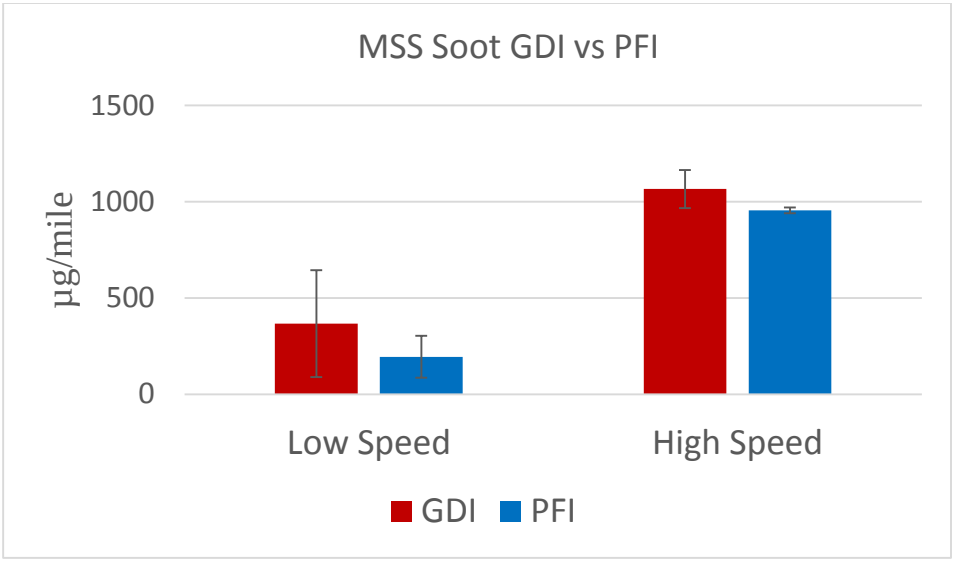

Figure 3-4.8 Photo-acoustic (MSS) soot comparison for a GDI and PFI vehicle

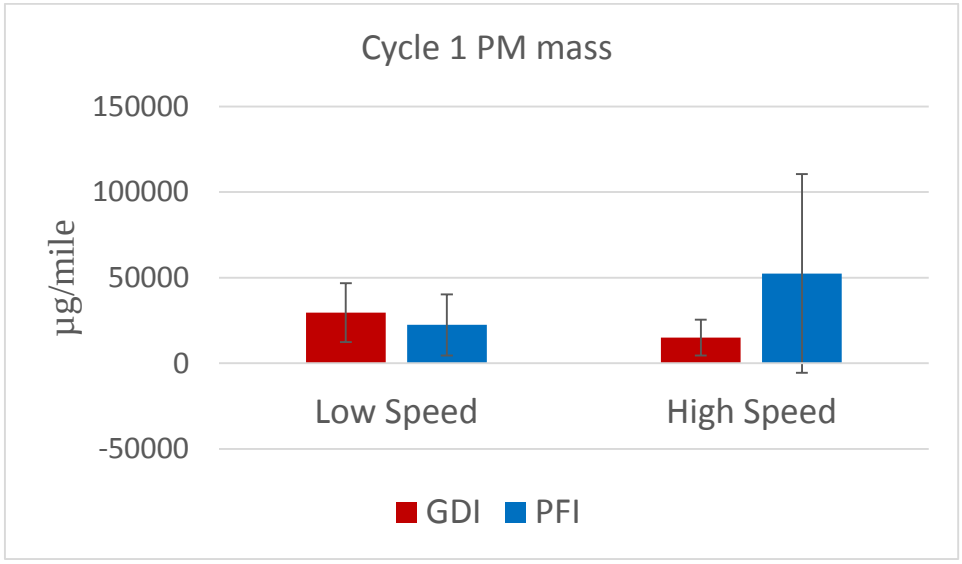

Figure 3-4.9 Filter soot mass comparison between a GDI and PFI vehicle.

3.5 Particle Size Distribution

In this study particle size distributions were taken using an engine exhaust particle sizer, TSI model 3090. The results show that both GDI and PFI vehicles exhibits higher particle count during higher speed driving. Moreover, the GDI vehicle has a larger accumulation mode during high speed driving than during low speed driving, indicative of higher solid particle count during high speed driving. Furthermore, the GDI vehicle has a larger accumulation mode than the PFI vehicle. While the PFI vehicle exhibited a larger nucleation mode during high speed driving than low speed driving, further indication of a high amount of volatile particles when the vehicle is subject to high speeds or high load. These can be seen in figures 3-5.1 and 3-5.2.

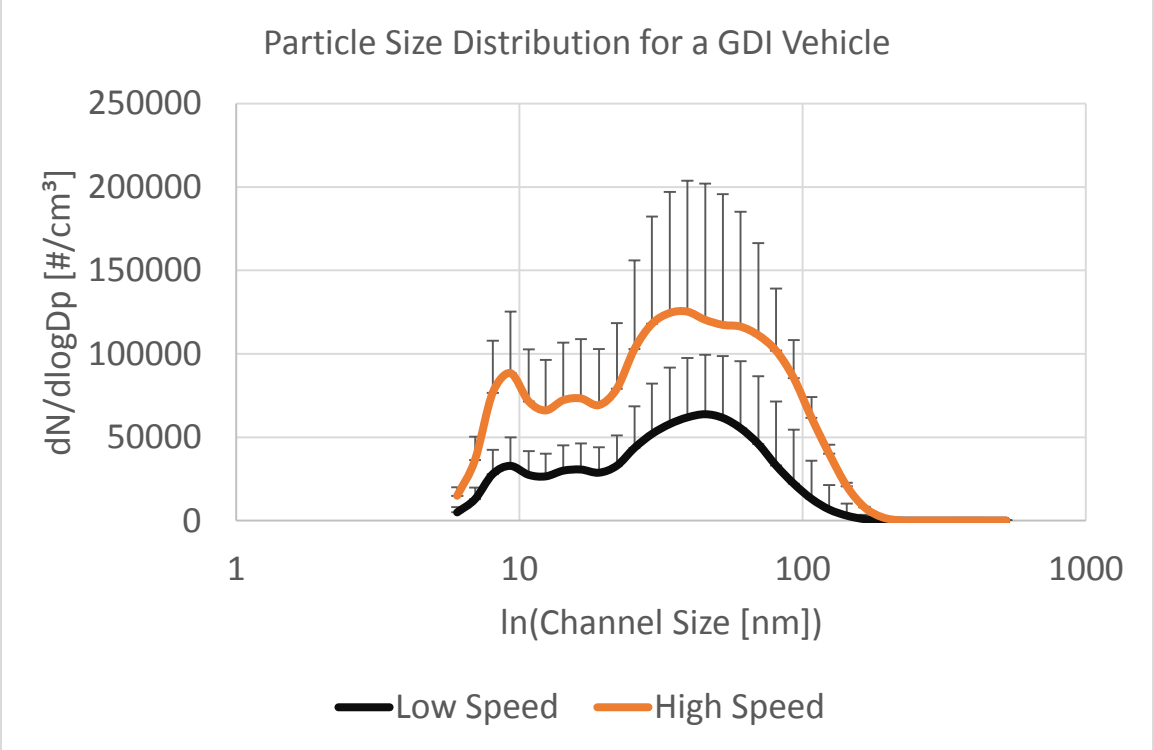

Figure 3-5.1 Particle size distribution for a GDI vehicle

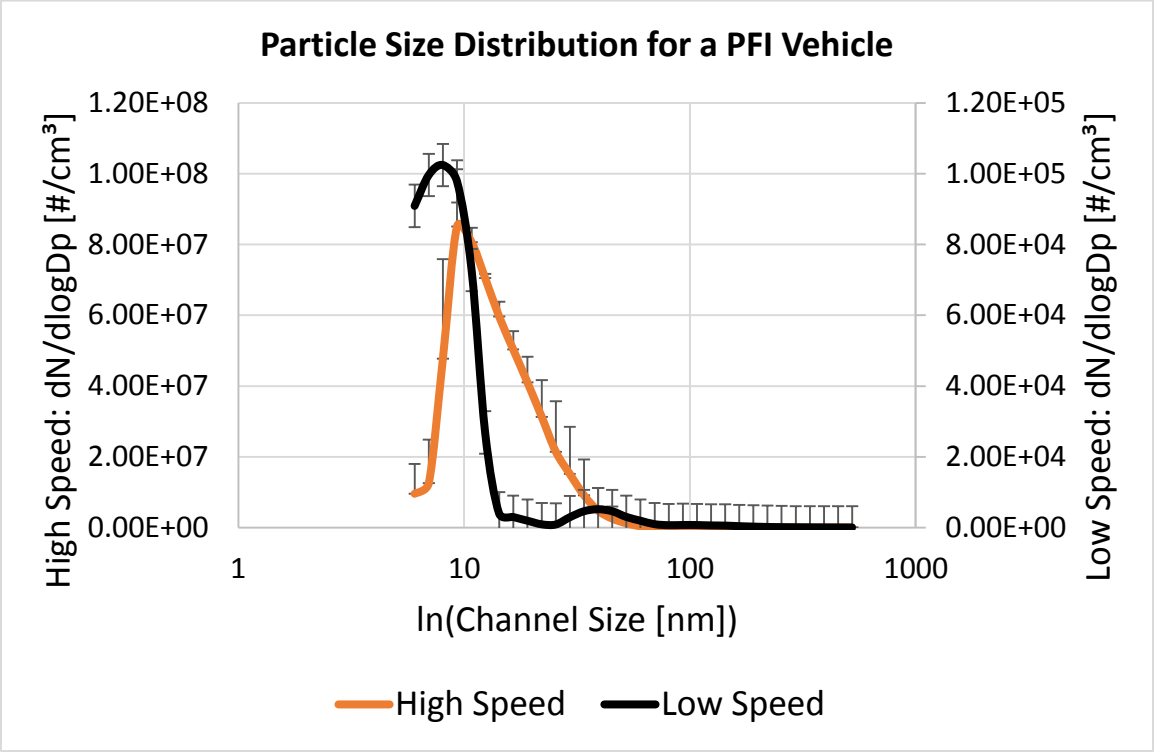

Figure 3-5.2 Particle size distribution for a PFI vehicle

4. Conclusion

Particle phase emissions from light-duty vehicles traveling at highway speeds remains largely misunderstood. This study aimed to understand emissions from various typical light-duty vehicles traveling at high freeway speeds in California. Data from the California Department of Transportation and the California Air Resources Board was used to compile specific vehicle classes as well as driving cycles that more accurately represent California's fleet today. These resulted in various vehicle emissions tests done at a unique and state-of-the-art chassis dynamometer lab facility. Both conventional, PFI, and emerging, GDI,

vehicle technologies were tested in an effort to understand future emission impacts from a dynamic fleet of vehicles. Overall the results show that high speed or high load influences vehicles of both technologies significantly. The results show that speed increases emissions significantly, this can be attributed to higher fuel consumption during high speed driving, furthermore, PFI vehicles were shown to have a larger total particle count than the GDI vehicles, which can be attributed to a high amount of volatile components present during high speed driving. Soot was also increased for high speed driving. Furthermore, GDI vehicles were shown to emit higher solid particles than PFI vehicles during both high and low speed driving. These results aim to aid future work on emission control strategies for emerging GDI engines and ultimately lower health effects of long term exposure to emissions.

5. References

1. National Highway Traffic Safety Administration. "2017-2025 Model Year Light-Duty Vehicle GHG Emissions and CAFE Standards: Supplemental." STP Standard temperature and pressure TC Torque converter TCC Torque converter clutch (2011).
2. Alson, Jeff. "Light-Duty Automotive Technology." EPA. Environmental Protection Agency, Dec. 2013. Web. 13 Nov. 2014
3. IPCC, 2013: Summary for Policymakers. In: Climate Change 2013: The Physical Science Basis. Contribution of Working Group I to the Fifth Assessment Report of the Intergovernmental Panel on Climate Change [Stocker, T.F., D. Qin, G.-K. Plattner, M. Tignor, S.K. Allen, J. Boschung, A. Nauels, Y. Xia, V. Bex and P.M. Midgley (eds.)]. Cambridge University Press, Cambridge, United Kingdom and New York, NY, USA.
4. Buckeridge, David L., et al. "Effect of motor vehicle emissions on respiratory health in an urban area." Environmental health perspectives 110.3 (2002): 293.
5. "Fuel Economy Survey | High Gas Prices - Consumer Reports." Fuel Economy Survey | High Gas Prices - Consumer Reports. N.p., n.d. Web. 25 Sept. 2014.
6. Çelik, Mustafa Bahattin, and Bülent Özdalyan. "Gasoline direct injection." *Fuel Injection, Sciyo* (2010).
7. Short, D., Vu, D., Durbin, T., Asa-Awuku, A. Components of Particle Emissions from Light- Duty Spark-Ignition Vehicles with Varying Aromatic Content and Octane Rating in Gasoline. Env. Sci. & Tech..
8. Spicher U., Kölmel A., Kubach H. and Töpfer G., Combustion in Spark Ignition Engines
9. with Direct Injection, SAE Paper 2000-01-0649.
10. Zhao, Fuquan, M-C. Lai, and David L. Harrington. "Automotive spark-ignited direct-injection gasoline engines." Progress in energy and combustion science25.5 (1999): 437-562.
11. Graskow, B., Kittelson, D., Abdul-Khalek, I., Ahmadi, M. et al., "Characterization of Exhaust Particulate Emissions from a Spark Ignition Engine," SAE Technical Paper 980528, 1998, doi:10.4271/980528.
12. "Welcome to Traffic Census." Traffic Census. N.p., n.d. Web. 01 Oct. 2014.
13. "Your Local Office." Caltrans ::. N.p., n.d. Web. 01 Oct. 2014.
14. Niemeier, Debbie, E. Douglas, and T. Kear. "The California Department of Transportation/Air Resources Board Modeling Program (CAMP): New Research to Improve Speed Correction Factors and Mobile Source Emissions Modeling."11th Annual Emission Inventory Conference. 2002.
15. Sierra Research, Inc. (2002a). Task Order No. 2: SCF Improvement – Field Data Collection. Prepared for California Department of Transportation, July 18.
16. Mordas, G., et al. "On operation of the ultra-fine water-based CPC TSI 3786 and comparison with other TSI models (TSI 3776, TSI 3772, TSI 3025, TSI 3010, TSI 3007)." Aerosol Science and Technology 42.2 (2008): 152-158.
17. TSI Incorporated. Ultrafine Condensation Particle Counter Model 3776. N.p.: TSI Incorporated, n.d. Print.

18. TSI Incorporated. The Engine Exhaust Particle Sizer Spectrometer Model 3090. N.p.: TSI Incorporated, n.d. Print.
19. AVL. AVL Micro Soot Sensor Transient High Sensitive Soot Measureme. N.p.: AVL, 2010. Print.
20. Petzold, Andreas, et al. "Evaluation of multiangle absorption photometry for measuring aerosol light absorption." Aerosol Science and Technology 39.1 (2005): 40-51.
21. Ntziachristos, Leonidas, et al. Use of a catalytic stripper as an alternative to the original PMP measurement protocol. No. 2013-01-1563. SAE Technical Paper, 2013.
22. Transportation Statistics Annual Report 2012. Rep. U.S. Department of Transportation, 2012. Web.
23. Feng, Y., V. Ramanathan, and V. R. Kotamarthi. "Brown carbon: a significant atmospheric absorber of solar radiation?." *Atmospheric Chemistry and Physics*13.17 (2013): 8607-8621.

Particle Phase Emission Reductions from an Ocean-Going Vessel Equipped with a Scrubber

1. Background

Globalization today is responsible for the large amount of raw materials and finished goods shipped all over the world by large ocean-going vessels (LOGVs). LOGVs represent one of the largest uncontrolled emission sources of smog and soot precursors, as these vessels are the last of the diesel engine sources to be controlled[1].

1.1 Black Carbon

Black carbon (BC) is characterized by the ability to strongly absorb visible light[3]. It is often formed from the incomplete combustion of fuels and is thus considered an anthropogenic emission. BC has an average atmospheric lifetime of a few weeks but can significantly modify the earth's energy balance. Hence, BC is a short-lived, climate forcing agent. Thus, the reduction of atmospheric BC emissions is being considered as a near-term mitigation strategy for climate impacts[3].

BC has both direct and indirect climatic effects. BC is a dominant absorber of solar radiation in the atmosphere. Furthermore, BC is transported over long distances and can mix with other aerosols to form transcontinental plumes of brown clouds[4]. Anthropogenic sources of BC are concentrated in the tropics where high solar irradiance occurs. BC's high absorption properties, regional distribution aligned with high solar irradiance, and the capacity to mix and form widespread brown clouds make the emissions of BC the second strongest contribution to global warming, trailing behind carbon dioxide[3]. Furthermore, the deposition of BC darkens snow and ice surfaces, contributing to accelerate melting of Arctic sea ice.

1.2 Emission Regulations

PM related deaths near ports has been correlated with shipping emissions. Accordingly, port authorities have promulgated control measures to limit emission exposure to the surrounding port communities and thus reduce the health impact on its residents. One of the more common regulations is the control of sulfur levels in the fuel. This is done by switching from a residual fuel oil to a distillate fuel[1]. However, this method can be expensive and undesirable by the shipping companies. In addition to the actions at the regulatory level, the ship owners, through organizations like the International Maritime Organization (IMO), have invested in resources to better understand the impact of shipping on both the regional and global environments. Their topics cover the gambit of environmental concerns, including the emerging issues associated with the release of Black Carbon (BC) from ships and the subsequent deposition on Arctic ice[2].

IMO has a Marine Environment Protection Committee (MEPC) whose perspective matches that of our current knowledge of climate change[2]. As a consequence, MEPC of IMO agreed to develop a work plan to address the impact of carbon emissions from ships and instructed the Sub-Committee on Bulk Liquids and Gases (BLG) to develop a definition for black carbon emissions from international shipping. The group is to consider measurement methods for BC by identifying the most appropriate method for measuring black carbon emissions from international shipping, investigate appropriate control measures to reduce the impacts of black carbon emissions from international shipping in the Arctic, and submit a final report to MEPC 65 in 2014.

1.3 Emission mitigation from ocean-going vessels

The International Maritime Organization (IMO) is an agency of the United Nations that promotes maritime safety. Ship emission rules are contained in the International Convention on the Prevention of Pollution from Ships, also known as MARPOL[5]. MARPOL, which includes Annex VI, contains two sets of emission and fuel quality requirements. The first set outlines global requirements and the second set has more stringent requirements applicable to ships in emission control areas (ECA). ECA can be designed to control for SOx, particulate matter (PM), NOx or all three. Currently there are four control areas, one of which is in North America, including most of the U.S. and Canada's coast. This area is designed to control for NOx and SOx emissions from ships.

IMO, port communities, and shipping companies share a goal: to lower the air pollution impact from ship exhaust[5]. One way to achieve this is to use fuels with a lower sulfur concentration, thus Annex VI regulations include caps on sulfur content of fuel to control SOx emissions, and indirectly PM. Currently there is no explicit PM emission limits[5]. Sulfur limits and implementation dates are illustrated in Table 1-3.1 and Figure 1-3.1 below.

Table 1-3.1 MARPOL Annex VI Global and ECA Fuel Sulfur Limits (ABS)

Low Sulfur Fuel		Operating Areas			
Requirements	Outside ECAs	Inside ECAs	EU Ports	California Coastal	US EPA Category 1 and 2 Vessels
Starting Year 1 January	% Sulfur in Fuel	% Sulfur in Fuel	% Sulfur in Fuel	% Sulfur in Fuel	% Sulfur in Fuel
2010	4.5	1.0	0.1	1.5 (0.5)	0.0500 (500 ppm)
2012	3.5	1.0[†]	0.1	1.0 (0.5)	0.0015 (15 ppm)
2014	3.5	1.0	0.1	0.1	0.0015 (15 ppm)
2015	3.5	0.1	0.1	0.1	0.0015 (15 ppm)
2020 (2025)	0.5	0.1	0.1	0.1	0.0015 (15 ppm)

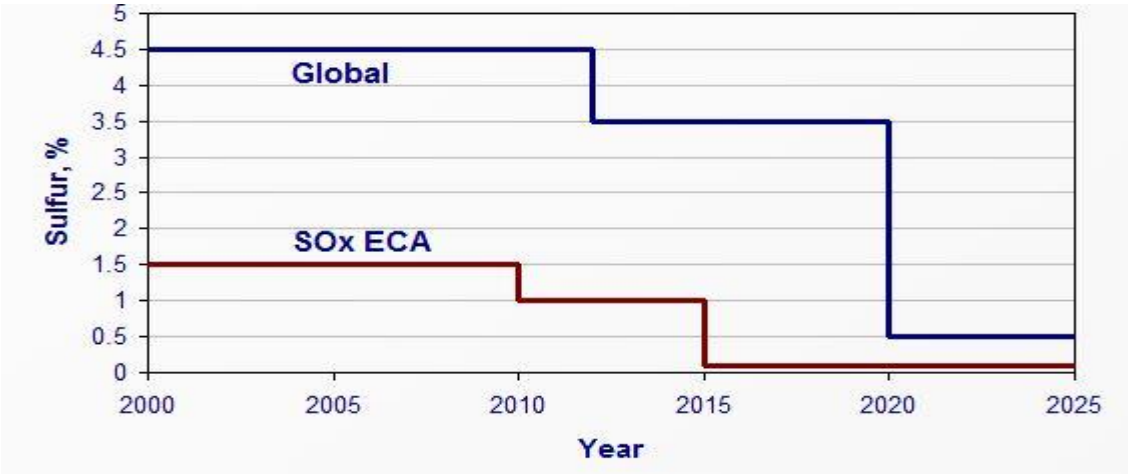

Figure 1-3.1 MARPOL Annex VI Global and ECA Fuel Sulfur Limits

Heavy fuel oil (HFO) is a commonly used fuel and is allowed provided it meets the sulfur limits. That is, a complete switch to distillate fuels is not required[5]. The processes required decrease sulfur content in fuel, are expensive, and thus there is an increase interest in achieving the goal through the use of scrubber technology. As shown in Table 1-3.1, in 2015, the ECA sulfur limit in fuel will be 0.1%. The SOx emission limits will require ships

to achieve a SOx reduction at least equivalent to a fuel with 0.1% sulfur or essentially >97% SOx removal by scrubbing, assuming a fuel with 3.5% sulfur[5].

Scrubber technology has been proven to be effective due to the large number of commercial installations[6]. However, there are a number of advocates who claim that the application of scrubber technology for the removal of gases and soot from the exhaust of diesel engines on ships is still in the learning phase because only few vessels have implemented such removal technology. The testimony in the Parliament Transport Committee, Evidence from Maritime UK (SES 03b), indicates issues when scrubbers are installed for commercial operation on ships.

For this study, the scrubber technology being tested is installed on the APL England, a 5,500 twenty-foot equivalent units (TEU) container vessel trading between Asia and the U.S. The system being tested is assumed to allow APL to continue using lower cost residual fuels, while reducing emissions, as per the IMO ECA rules. The scrubber is expected to reduce 80-85% diesel PM emissions, 99.9% SOx emissions, more than 90 percent of volatile organic compounds (VOC) and up to an additional 10 % reduction in NOx[7].

1.4 PM Control a scrubber approach

The APL England is equipped with three similarly sized, fixed RPM engines[11]. The scrubber system designed for this auxiliary engine includes three venturi PM impaction zones and one PM removal zone[11]. Thus, each engine is equipped with a separate venture impaction zone, yet the combined engine exhaust manifold supports the three engines.

Scrubber systems are air pollution control devices used on various industrial applications as a way to remove particles and gases from exhaust streams[8, 11]. See Figure 1-4.1.

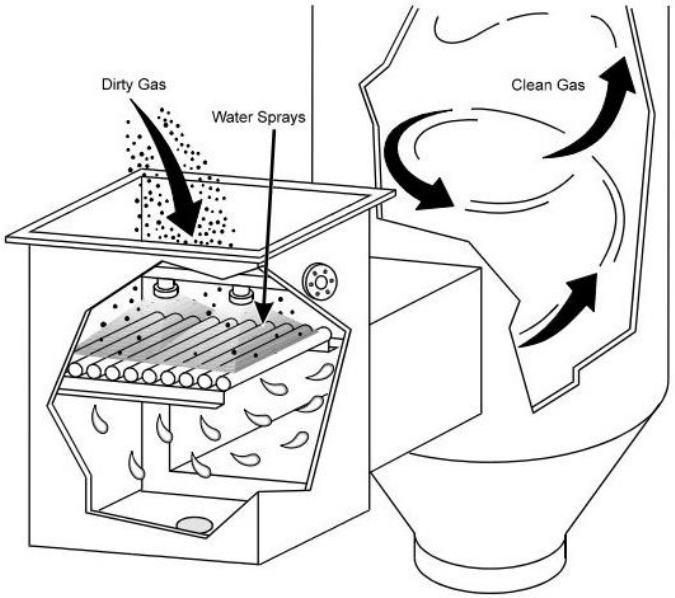

Figure 1-4.1 Scrubber system[12]

Scrubbers are one of the primary devices used to control gaseous emissions[8,12]. There are many configurations of web scrubbers and scrubber systems. Moreover, a wet scrubber describes a scrubber that uses liquids to remove pollutants. Wet scrubbers remove particles by capturing them into liquid droplets. Gases are removed by dissolving or absorbing them into the liquid[8, 12]. In this case, dirty industrial exhaust streams are brought in contact with the scrubbing liquid by forcing it through a pool of such liquid or through a liquid spray system[12]. These provide good contact between the liquid and exhaust stream. The scrubber used in the APL England is a venturi scrubber design[11], which can be seen in Figure 1-4.2. Under this configuration, another device called the entrainment separator is used to

separate any droplets that are in the flue gas from the clean exhaust. Moreover, in a venturi scrubber set up, the entrainment separator is called a cyclonic separator[12].

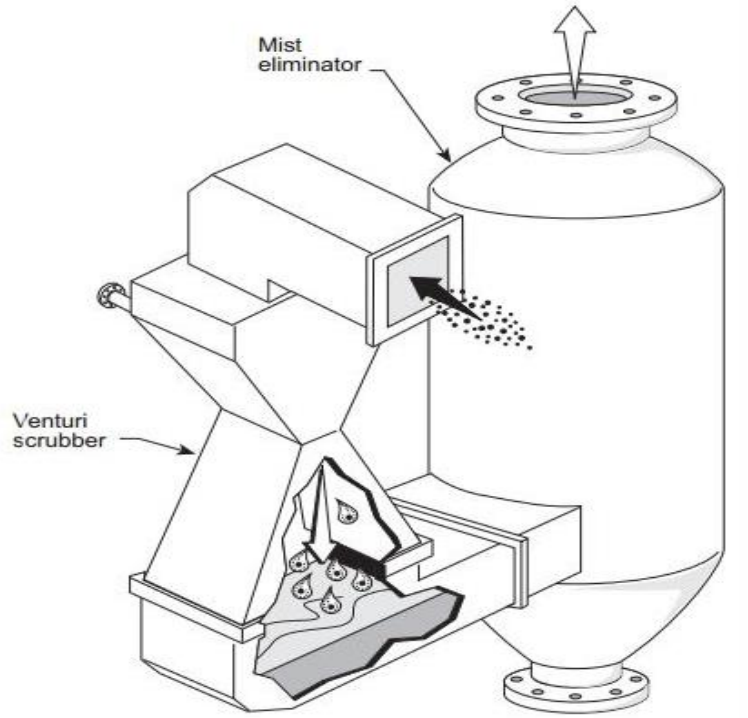

Figure 1-4.2 A venturi scrubber design[12]

This venturi scrubber is designed to achieve high particle collection efficiency[12]. This consists of three main sections: a converging section, a throat section, and a diverging section, as shown in Figure 1-4.2. The industrial exhaust enters the venturi through the converging section and then passes through a narrower throat. A liquid solvent is then added at the entrance of the converging section just before the throat section. This is very effective at handling hot exhaust and gas containing dust[12]. Then the exhaust gas traveling at high velocity is forced through the small throat section and shears liquid from the walls. This produces a big quantity of small liquid droplets. Particles and gases in the exhaust are removed as they mix with the fog of liquid droplets in the throat section. Finally, the

exhaust stream exits through the diverging section which has a larger area than the throat and is forced to slow down, as shown in Figure 1-4.3.

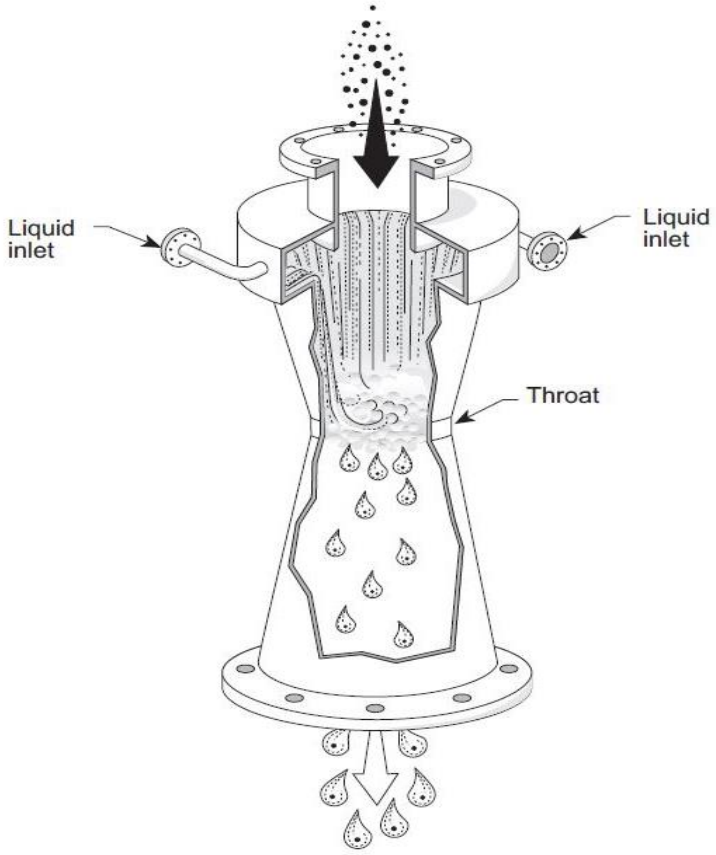

Figure 1-4.3 A venturi scrubber design[12]

Through this design, particle removal efficiency may be increased with increasing pressure drop. This is because of increased turbulence due to high exhaust velocity in the throat[13]. (Through this design, particle removal efficiency may be increased with increasing pressure drop from increased turbulence due to high exhaust velocity in the throat.) A venturi scrubber is typically operated with pressure drops ranging from 2 to 60 in of water[13]. Furthermore, the solvent liquid injection rate can also affect particle collection. An

appropriate amount of solvent must be added to the throat in order to provide adequate wall coverage. Particle capture efficiency may dramatically decrease as a result of insufficient liquid coverage[14, 15]. A schematic of the APL England PM scrubber system is shown in Figure 1-4.4. This shows three main impaction zones where PM is removed by entering the venturi at high velocities. The water is then discarded through water discarding spray system[11]. The engine emission sampling occurred on one of the three auxiliary engines. The pre-scrubber sample point was one of the three exhaust stacks labeled Emissions Test Ports In. This was on the highest point of the ship several decks above the observation deck. The post-scrubber sample was collected from the stack after the three engines' exhausts were combined, labeled Emissions Test Out.

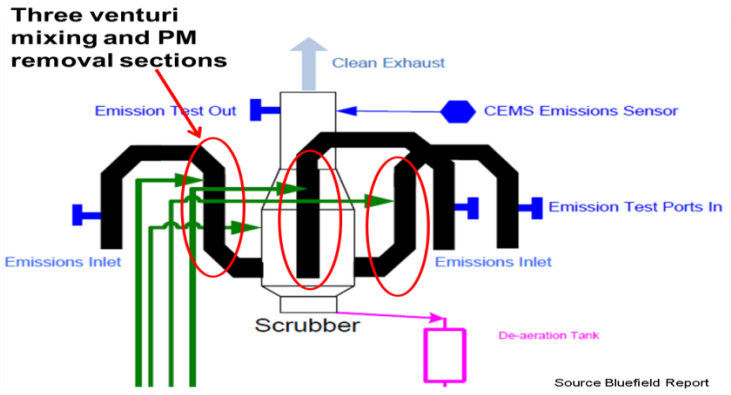

Figure 1-4.4 APL England scrubber system[11]

3. Experimental set-up

The measurement approach closely followed the International Organization for Standardization (ISO) protocol methods. The ISO 8178 is an international standard for

measuring exhaust emissions from various off-road engine applications[9, 10]. ISO 8178-1 and ISO 8178-2 specify the measurement and evaluation methods for gaseous and particulate exhaust emissions when combined with combinations of engine load and speed provided in IS0 8178- Part 4: Test cycles for different engine applications.

3.1 Testing Protocol

The selected auxiliary engine tested is a 3.2 MW Samsung-MAN B&W engine, model 7l32/40, including a generator manufactured by Hyundai. The APL England has 3 main auxiliary engines and each is configured with a scrubber[11]. Table 3-1.1 provides technical specifications of the selected engine. Table 3-1.2 provides information on the various loads tested. 6 modes were tested pre and post scrubber overall. Each during high, medium and low loads and Table 3-1.3 is a fuel report provided by the APL England, in which the sulfur content used is below 1% by mass.

Table 3-1.1 Summary of selected auxiliary engine specifications

Description	Value	Units
Rated power	3265	kW
Electrical rating	2900	kW
Displacement	218.19	liters
Engine speed	720	RPM

Table 3-1.2 Test matrix for the tested auxiliary engine

Nominal Load	Location	Load e_kW	Actual Load %	Exhaust flow [3] scfm	Nm3/min	ACONIS-PMS [2] e_kW	stdev kW	Engine Intake P_bar	T_C	Fixed [1] RPM
Mode 1	Post	1689	58.2%	6095	172.6	1689	31.5	1.65	42	720
Mode 2	Post	1279	44.1%	5164	146.2	1279	48.6	1.24	42	720
Mode 3	Post	595	20.5%	3740	105.9	595	8.4	0.61	41	720
Mode 1	Pre	1602	55.2%	5909	167.3	1602	2.1	1.57	42	720
Mode 2	Pre	1243	42.9%	5004	141.7	1243	11	1.17	42	720
Mode 3	Pre	603	20.8%	3720	105.3	603	2.1	0.61	42	720

Table 3-1.3 Auxiliary engine test fuel report provided by the APL England

Parameters	Test Results	Units
Density @ 15C	986.0	kg/m^3
Viscosity @ 50C	163.2	cSt
Sulfur	0.92	% (mass)
Viscosity @ 100C	20.7	cSt
API Gravity	11.93	
Net Specific Energy	40.88	MJ/kg
Gross Specific Energy	43.22	MJ/kg

3.3 Testing Set Up

A well designed sampling system is important to accurately collect sample exhaust. Testing on the APL England followed standard ISO practice for on-vessel emissions testing. A schematic of ISO 8178-2 can be seen in Figure 3-3.1.

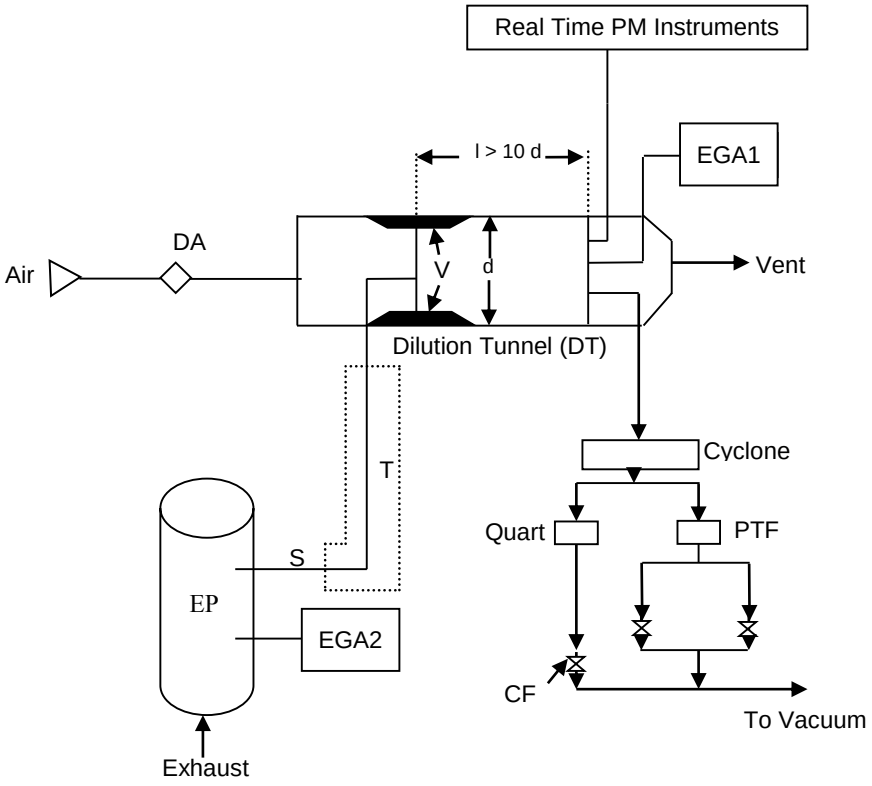

Figure 3-3.1 ISO method for on-vessel emissions testing sample schematic

ISO 8178-1 and ISO 8178-2 specify methods for gaseous and particle exhaust emissions used in tandem with varying engine load and speeds as provided in ISO 8178 – Part 4: Test cycles for different engine applications. This method uses a partial flow dilution system with a venturi. PM measurement studies conducted have determined that moderate PM loss can be attributed to long transfer lines[16]. Thus, for this study, heated transfer lines have been eliminated as an effort to reduce PM loss; hence, direct sampling was done from the ship's exhaust. This resulted in longer startup times since the instrumentation needed to be at the sample location, which in this case was five stories above the main ship deck. As Figure 2-3.1 shows, raw exhaust is sampled from the exhaust pipe (EP) through a sample

probe to a dilution tunnel (DT). This occurs due to negative pressure created by the venturi phenomenon. Figure 3-3.2 shows the dilution system and measurement layout on one of the auxiliary engine exhaust stack.

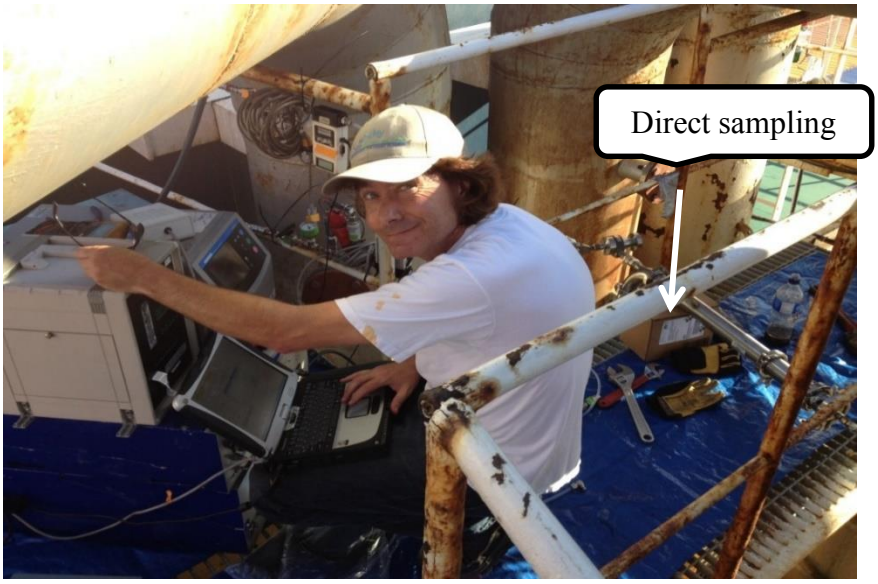

Figure 3-3.2 Measurement layout on auxiliary engine exhaust

3.4 Particulate Matter Measurement Techniques

PM measurements were taken using a myriad of techniques. Samples were collected using Whatman Teflo filters for total PM and Quarts fiber filters for composition. Both used the NIOSH and IMPROVE analytical methods for offline laboratory analysis. Real time instruments were also used to measure black carbon emissions. These were AVL's micro-soot sensor (MSS) model 483, the Thermo Scientific Multi-Angle Absorption Photometer (MAAP) model 5012, and Magee Aethalometer (AE33) model AE33. These instruments along with their measurement techniques are outlined in Table 3-4.1.

Table 3-4.1 Measurements utilized and their measurement principle[24]

Instrument	Model	Principle	Output	Wavelength
Micro Balance	UMX2	Gravimetric net weight change	Total $PM_{2.5}$ measurement	-
Sunset Laboratory Carbon analyzer	Lab OC-EC	Flame Ionization Detection (FID)	Operationally defined organic and elemental carbon via transmittance	-
Micro Soot Sensor (MSS)	MSS 483	Photo-acoustic (PA)	BC mass from real time in-situ signal (mg/m^3)	808 nm
Mutli-Angle Absorption Photometer (MAAP)	MAAP 5012	Aerosol absorption	BC mass from transmissions and scattering correction ($\mu g/m^3$)	670 nm
Aethalometer	AE33	Filter paper transmission	BC mass from transmission ($\mu g/m^3$)	370, 470, 520, 590, 660, 880, and 950

It is important to note that black carbonaceous material is reported based on its measurement technique[3]. There are various measurement techniques available and the terminology can be mixed. The terms black carbon, elemental carbon and soot refer to the light-absorbing particle components yet their measurements can differ. Thus, different BC measurement techniques are important to learn about the nature and quantity of exhaust BC.

BC measurement instrumentation includes optical, thermal or incandescence methods[17]. BC inventories are based on emission factors derived from thermal-optical methods. These detect BC evolving from a heated filter sample. On the other hand, atmospheric monitoring stations use optical absorption methods to measure BC[18]. The MAAP, Aethalometer and PA-soot all measure BC from light-absorption measurements. The MAAP and

Aethalometer use filter based methods to measure and report BC continuously. PA-soot is a photo-acoustic measurement which measures the intensity of a sound wave generated by the contraction and expansion of gas molecules when BC is pulsed by a laser[19]. This method then uses a conversion factor derived from gravimetric methods to soot content. PA-soot based BC has the largest range of measurement and can measure up to 50,000 $\mu g/m^3$, while the MAAP and Aethalometer can measure up to 100 $\mu g/m^3$.

3.5 Quality Control

Quality control is an important factor attributing to data validation in off-road emissions measurements. This section describes the standard practices used for calibration, verification and control checks performed before, after and during testing.

Prior to loading and packing instrumentation all systems were verified and cleaned. The MAAP, Aethalometer, and PA systems were all prepared for the testing campaign by verifying system specifications. The PA system was cleaned and verified to be up to specification by cleaning the internal pollution window and performing a span calibration using an internal pollution window. NIST traceable calibration tanks were used to perform pre- and post-test calibrations. Zero checks for all PM instruments were performed hourly throughout the duration of the test. Prior to each sample point, leak checks were performed for the PM system. The dilution ratio was verified at the conclusion of the test campaign by removing the sample probe from the dilution tunnel placing it in the exhaust pipe and measuring directly. This was used in addition to operating two gas analyzers.

Brake-specific fuel consumption was verified with reported manufacturer specifications. These were done in an effort to validate the data collected on the APL England auxiliary

engine out emissions was accurate and representative of the functioning system. This involved corresponding with the engine manufacturer to discuss the emission basis results. The brake-specific fuel consumption results were within reason of manufacturer specifics and thus suggest emission data collected was valid.

4. Results

Emission results for the test campaign on the APL England's auxiliary engines equipped with a scrubber PM reduction system are organized in three sections: Regulated Emissions, PM Emissions and Scrubber Performance.

4.1 Regulated Emissions

Regulated emissions (PM, NOx, CO_2) for the auxiliary engine are shown as a function of time in Figure 4-4.1. Per the test campaign, the post-scrubber exhaust was sampled and tested first immediately followed by pre-scrubber exhaust. Dilute NOx, CO_2 and PM concentrations varied from 100 – 300 ppm, 1.5% – 2.5% and 0.3 mg/m^3 – 3 mg/m^3, respectively.

The stars in Figure 2-4.1 indicate when filter batch Teflon and Quartz filter media were collected. Three batch samples are ideal. However, due to time constraints some tests only collected two filter samples. Figure 4-4.1 also shows large spikes in the gaseous emissions, which are a result of dilution ratio quantification. It is important to note that the system experienced a data recording glitch starting at 11:00 A.M. to 12:20 P.M. During this time

the system did not record real-time gaseous emissions data. Hand records were instead utilized to record the data. These records indicate that NOx and CO_2 concentrations were stable. PA-soot measurements showed to be unstable during mode 3, which is when the engine is running at its lowest load mode. The engine was stabilized under this mode for well over an hour and it is unclear what caused this instability to occur.

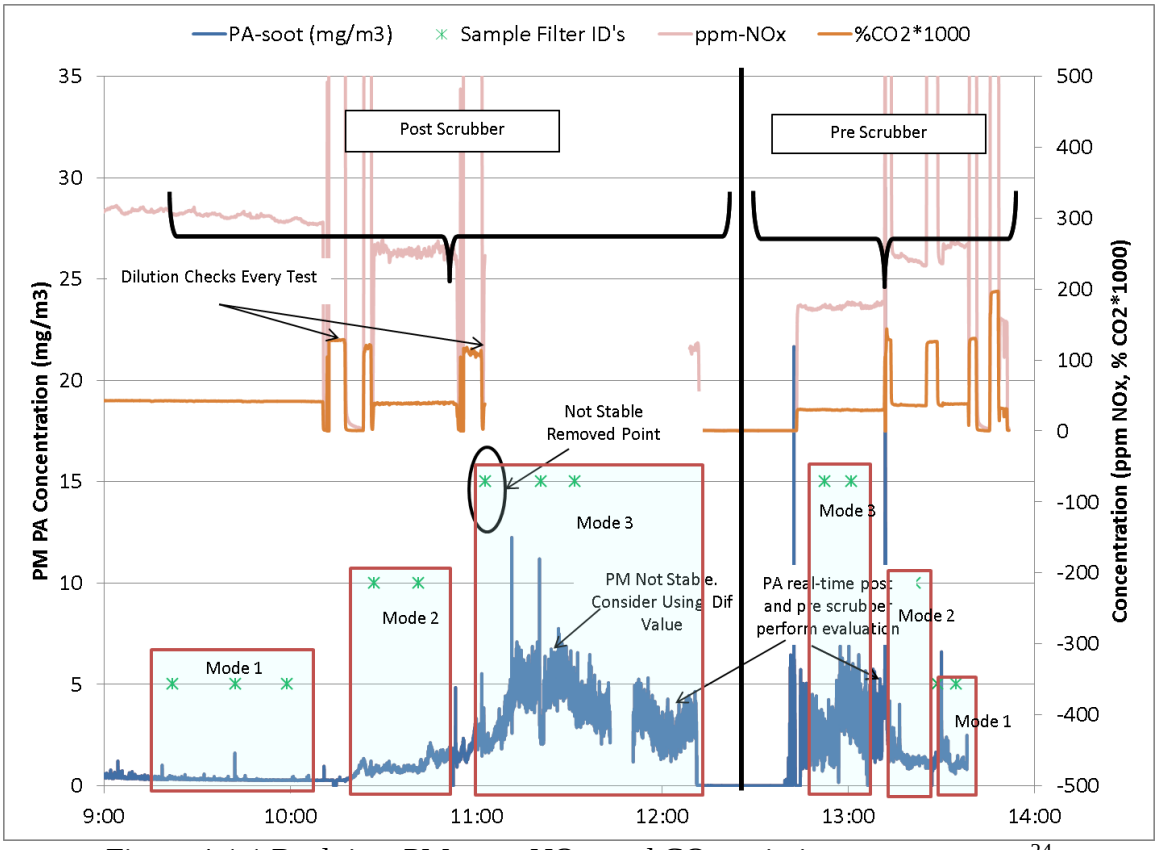

Figure 4-1.1 Real time PM-soot, NOx, and CO_2 emission measurements[24]

Brake-specific regulated emission results are tabulated in Tables 4-4.1 and 4-4.2. Engine load was varied, ~60% - 20% for pre- and post-scrubber tests. The results show that the brake-specific NOx (bsNOx) emissions were stable during all engine loads for both pre-

and post-scrubber test points. bsNOx emission was calculated and averaged to 10.3 g/kWhr. CO_2 brake-specific emissions ($bsCO_2$) were calculated to be 720 g/kWhr during high load and 820 g/kWhr during low load. These values agree with published literature data where higher brake-specific fuel consumption at low loads is present. Furthermore, $bsCO_2$ emission results were similar for pre- and post-scrubber test points, suggesting the two test conditions agree.

Table 4-1.1 Brake-specific emission results for the aux. engine (g/kWhr basis)

Nominal Load	eLoad e_kW	Load %	NOx g/kWh	CO g/kWh	CO2 g/kWh	$PM_{2.5}$ mg/kWh	PA-soot mg/kWh
Post M1	1689	58.2%	10.79	0.62	717.8	206.2	5.6
Post M2	1279	44.1%	9.76	0.89	719.1	199.5	22.2
Post M3	595	20.5%	10.75	1.63	819.7	294.4	88.2
Pre M1	1602	55.2%	10.66	0.83	752.2	407.6	28.6
Pre M2	1243	42.9%	10.90	0.99	781.8	373.3	32.5
Pre M3	603	20.8%	9.99	2.05	805.2	491.1	90.5

Table 4-1.2 Time specific emission results for the aux. engine (g/hr basis)

Nominal Load	eLoad e_kW	Load %	NOx kg/hr	CO kg/hr	CO2 kg/hr	SO2 kg/hr	$PM_{2.5}$ g/hr	PA-soot g/hr
Post M1	1689	58.2%	18.22	1.04	1212	0.066	348.2	9.4
Post M2	1279	44.1%	12.48	1.13	920	0.056	255.2	28.4
Post M3	595	20.5%	6.40	0.97	488	0.045	175.3	52.5
Pre M1	1602	55.2%	17.07	1.32	1205	2.288	652.8	45.9
Pre M2	1243	42.9%	13.55	1.23	972	1.897	464.0	40.4
Pre M3	603	20.8%	6.02	1.24	485	0.955	295.9	54.5

4.2 $PM_{2.5}$ and Organic Carbon (OC)

Brake-specific PM (bsPM) emissions were calculated for pre- and post-scrubber test points. These results are tabulated in Table 2-4.3 Total PM measurements include $PM_{2.5}$ and EC/OC PM from the NIOSH and IMPROVE methods. The results show that engine

out bs$PM_{2.5}$ ranged from 491 mg/kWhr at light load to 400 mg/kWhr at high load. Higher bs$PM_{2.5}$ emissions at low loads agree with typical diesel marine engine emission rates[16]. NIOSH OC PM was calculated to be higher than IMPROVE OC PM. The NIOSH OC PM ranged from 183 mg/kWhr to 296 mg/kWhr where the IMPROVE OC PM ranged from 158 mg/kWhr to 173 mg/kWhr for equivalent engine load conditions. The results show that the NIOSH OC PM method was upwards of 40% higher than the IMPROVE method at the low load test condition. Marine engines typically burn high sulfur fuels[7], e.g. marine fuel oil (MFO). These tend to have PM exhaust that is dominated by OC and sulfate[16]. EC + OC masses were ~50% of total $PM_{2.5}$. Although sulfate PM was not directly measured, this can be inferred from SO_2 concentrations in the exhaust[16]. The difference in $PM_{2.5}$ and the sum of EC and OC is approximately the sulfate PM mass. Thus, total PM composition is 45% sulfate, 45% organic carbon and 10% elemental carbon, which is in agreement with previous studies[16].

Table 4-2.3 Total PM, BC, and EC/OC brake-specific PM emissions

					NIOSH		IMPROVE			
Nominal Load	eLoad e_kW	Load %	$PM_{2.5}$ mg/kWh	PA-soot mg/kWh	EC mg/kWh	OC mg/kWh	EC mg/kWh	OC mg/kWh	MAAP mg/kWh	Aeth mg/kWh
Post M1	1689	58.2%	206.2	5.6	3.68	79.6	8.35	74.8	n/a	n/a
Post M2	1279	44.1%	199.5	22.2	14.13	82.6	27.55	74.6	n/a	n/a
Post M3	595	20.5%	294.4	88.2	99.09	126.9	133.15	95.5	n/a	n/a
Pre M1	1602	55.2%	407.6	28.6	29.69	257.8	35.21	166.8	n/a	n/a
Pre M2	1243	42.9%	373.3	32.5	27.98	183.0	40.71	158.1	n/a	n/a
Pre M3	603	20.8%	491.1	90.5	n/a	295.8	n/a	173.2	n/a	n/a

4.3 Black Carbon

Elemental carbon and black carbon are measured with varying techniques and principles[17]. Despite their correlations, some scientists reject the motion that EC emissions can be representative of BC emissions. Thus, it is desired to evaluate BC emissions from various measurement techniques. For this study, BC measurements were made using both the absorption photometer and photo-acoustic techniques. The results show that EC measurements are in agreement with PA-Soot measurements for both the NIOSH and IMPROVE methods. Both EC PM and PA-Soot ranged from 5 mg/kWhr at high engine load to around 100 mg/ kWhr at low engine loads.

The MAAP and Aethalometer both measure BC indirectly, yet they should correlate with the PA-soot measurements. This correlation is expected to incur varying levels of measurement bias and thus a perfect correlation is not expected[22].

The MAAP and Aetalometer PM have a maximum detection limit[20,21] of 0.1 mg/m^3. This is a great application for low ambient concentrations less than 0.01 μg/m^3. For this study, the soot concentrations were well above 0.1 mg/m^3, approximately 0.3 mg/m^3, thus both the MAAP and Aethalometer reached their detection limits and over-ranged. As a result, both these instruments did not provide valid BC data for the entire testing campaign. Higher dilution would be required for these instruments to measure BC within their range. For this study, the dilution ratio averaged around 3.5 where a dilution ratio of 200 to 1 is recommended when using these instruments.

Measurements of $PM_{2.5}$, OC and SO_2 did not show an increasing trend. At high load and low load, these measurements showed reductions. Suggesting that the PM measurement

instability only occurred for EC and BC measurements during 11:00 AM and 12:30 PM. This a drawback of batch measurements not experienced in real-time measurements. At 11:50 AM the PA-soot measurements were stable and used to evaluate the post-scrubber PM removal performance.

4.4 Scrubber Performance

PM was measured pre- and post-scrubber. The data in Table 4-4.1 shows PM reductions across the scrubber. All measurement methods indicated a PM post-scrubber reduction. Negative percentages represent a reduction in PM. A range of $PM_{2.5}$ reduction was calculated to vary between 50% at high load and 40% at low load. OC PM was also reduced, with both the NIOSH and IMPROVE method displayed reductions ranging from 69% to 55% and 55% to 45%, respectively. Both OC PM methods agree, showing a high reduction in PM post-scrubber at high loads.

Table 4-4.1 Scrubber PM emission reductions

Engine Conditions			Real Time			Gravimetric	NIOSH		IMPROVE	
Nominal Load	eLoad e_hp	Load %	PA-soot %	MAAP %	Aeth %	$PM_{2.5}$ %	EC %	OC %	EC %	OC %
M1 Effic	1645	57%	-81%	n/a	n/a	-49%	-88%	-69%	-76%	-55%
M2 Effic	1261	43%	-32%	n/a	n/a	-47%	-49%	-55%	-32%	-53%
M3 Effic	599	21%	-3%	n/a	n/a	-40%	n/a	-57%	n/a	-45%

PA-soot PM displayed a reduction range of 81% to 3% for high and low engine loads. Upon applying statistical analysis to the data set, the standard deviation of the low load measurement discredited any reduction in PA-soot PM. Again, EC and PA-soot measurements have been documented to correlate well[14]. This also occurs in this study,

where EC reductions were similar to PA-soot. EC was reduced across both the NIOSH and IMPROVE methods and was about 80% at high loads and less at low loads.

Figure 4-4.1 shows pre- and post-scrubber particulate matter (PM), photo -acoustic soot (PA-soot).

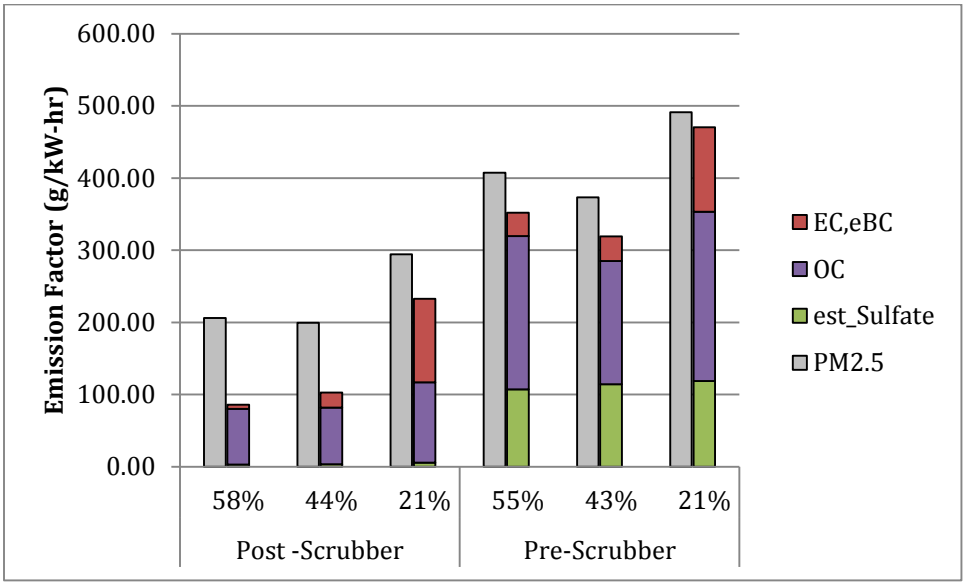

Figure 4-4.1 PM, BC, and EC/OC emission factors[24]

Figure 4-4.2 shows a PM reduction across the scrubber by all measurement methods. PA-soot PM showed a reduction from 81% at high load to 3% at light load, suggesting that the scrubber does not reduce BC at light loads as it does at high loads.

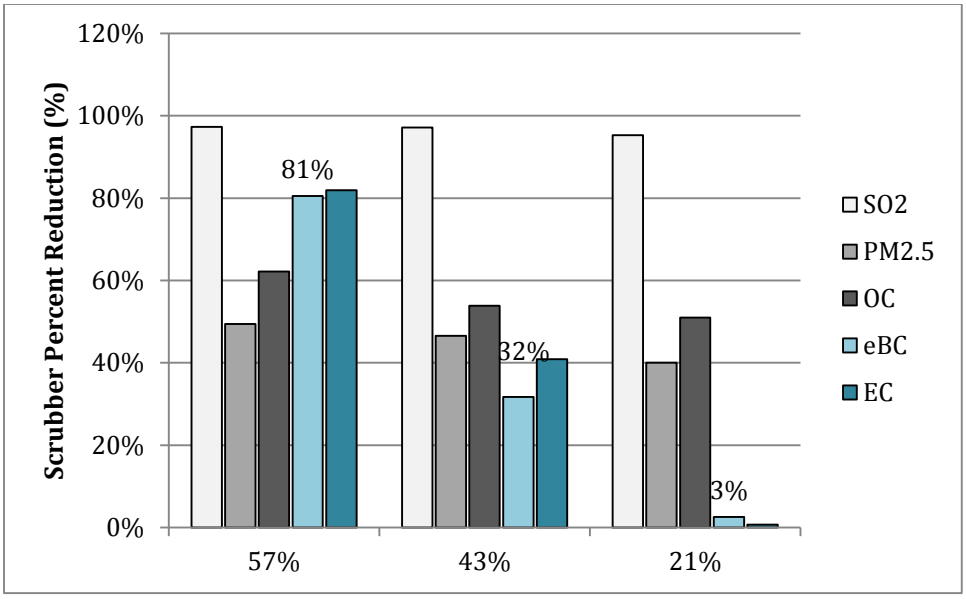

Figure 4-4.2 Gas and PM scrubber reductions[24]

The results show that this properly operated PM scrubber system fails to reduce BC at low load compared to high load engine conditions. This is suggested through the valid PA-soot measurements, which remained stable throughout most of the study. EC and BC reduction by scrubbers is based on the principles of impaction and diffusion[12]. For this scrubber system, for small particles (<100nm) to be removed they must travel at sufficient velocity in the venturi impaction zone. At low loads, these small particles experience low Reynolds number fueled by low velocity. This creates low turbulence in the venturi impaction zone and thus may not be enough to remove such particles. Hence, BC removal efficiency is dramatically reduced when engines are operating at low load conditions as shown by this study.

This work suggests scrubber performance and efficiency should be accompanied by operator education to maximize its reduction capabilities. Typically, diesel engines are not designed to operate under low load conditions. This is as an effort to maximize fuel

economy and efficiency. Low load conditions may be avoided as an effort to increase BC removal efficiency.

5. Black Carbon Measurement Recommendations

This test campaign included researching and providing recommendations for BC sampling and measurement approaches for off-road engines. The current standard approach to sample and measure $PM_{2.5}$ is described in ISO 8178. This approach requires condensation and temperature control achieved by a dilution tunnel. ISO 8178 recommends a minimum dilution of 4 to 1 as well as accurate verification[9,10]. This study's measurement approach to sample and measure BC was to use the same guidelines underlined in ISO 8178 for $PM_{2.5}$. Under these conditions, the PA-soot BC instrument worked well and no additional modifications are recommended. Unlike the PA-soot BC instrument, the MAAP and Aethalometer did not work well under such guidelines, thus recommendations can be made. An additional dilution as high as 200 has been estimated to be sufficient for the MAAP and Aethalometer to operate within their detection range. To achieve such high dilution accurate flow measurements are required per ISO 8178.

Figure 5-1.1 displays a simplified layout of ISO 8178 procedures for engine exhaust sampling. A small update is recommended to modify BC ISO 8178 to ensure proper sampling techniques and valid data. There is no procedure change for PA-soot instruments and other high concentration capable instruments.

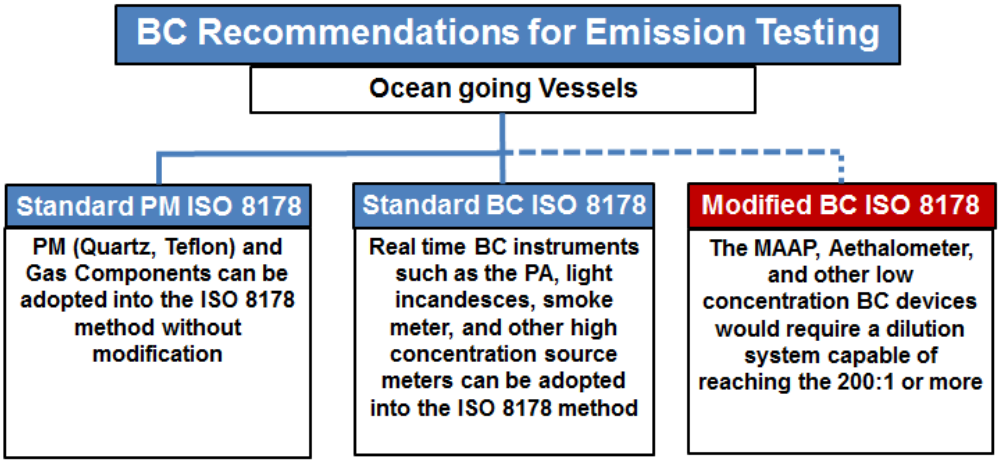

Figure 5-1.1 BC sampling recommendations for off-road engine exhaust testing

6. Conclusion

Off-road emissions testing can be challenging and complex, not all tools are readily avaialbe and thus heavy planning is necessary. During this study black carbon and regulatory emissions were sampled, measured and characterized from an auxiliary engine equipped with a PM control device, a scrubber. Scrubber performance was based on SOx, NOx, CO_2, THCs, and PM ($PM_{2.5}$, EC, OC and BC) characterization. Several real-time and batch measurements were utilized to sample engine exhaust. Existing ISO 8178 sampling guidelines are well suited for high concentration capable instruments while low concentration detection limits for ambient instruments would require a slight ISO 8178 change.

In summary, BC measurements were successful for real-time PA-soot type instruments but failed for batch type systems, which reached their detection limit caused by high BC concentration in exhaust streams. PA-soot, EC-NIOSH, EC-IMPROVE all showed similar PM reduction efficiency at both high and low load engine conditions. Furthermore, brake-

specific CO_2 emissions agree with typical values for large displacement steady-state diesel generators, suggesting valid test conditions and thus data was recorded. A 96% reduction in SOx was observed, which further suggests tests validation per expected SOx performance for scrubbers[23]. The OC-NIOSH method displayed higher OC reduction than the IMPROVE method. Scrubbers do not achieve high BC reduction when operating under low load engine conditions.

7. References

1. Agrawal, Harshit, et al. "In-use gaseous and particulate matter emissions from a modern ocean going container vessel." Atmospheric Environment 42.21 (2008): 5504-5510.
2. Becker, Rebecca. "MARPOL 73/78: An Overview in International Environmental Enforcement." Geo. Int'l Envtl. L. Rev. 10 (1997): 625.
3. Petzold, A., et al. "Recommendations for reporting" black carbon" measurements." Atmospheric Chemistry and Physics 13.16 (2013): 8365-8379.
4. Martins, J. Vanderlei, et al. "Effects of black carbon content, particle size, and mixing on light absorption by aerosols from biomass burning in Brazil." Journal of Geophysical Research: Atmospheres (1984–2012) 103.D24 (1998): 32041-32050.
5. Annex, V. I. "of MARPOL 73/78, Regulations for the prevention of air pollution from ships and NOx technical code." IMO London (1998).
6. Licht, William. Air pollution control engineering: Basic calculations for particulate collection. Vol. 10. CRC Press, 1988.
7. Ellman, Louise. Sulphur emissions by ships: sixteenth report of session 2010-12, Vol. 1: Report, together with formal minutes, oral and written evidence. Vol. 1. The Stationery Office, 2012.
8. Bellas, Allen S. "Empirical evidence of advances in scrubber technology."Resource and Energy Economics 20.4 (1998): 327-343.
9. International Standards Organization, IS0 8178-1, Reciprocating internal combustion engines - Exhaust emission measurement -Part 1: Test-bed measurement of gaseous particulate exhaust emissions, First edition 1996-08-l5
10. International Standards Organization, IS0 8178-2, Reciprocating internal combustion engines - Exhaust emission measurement -Part 2: Measurement of gaseous and particulate exhaust emissions at site, First edition 1996-08-l5
11. Bluefiend Incorporated. Evaluation of the Emission Reduction Performance of a Hamworthy/Krystallon Exhaust Gas Cleaning Scrubber. Rep. N.p.: n.p., n.d. Print.
12. EPA (1998) Lesson 2: Operating Principles of Scrubbers, EPA document 2.0-7/98
13. Brady, J. D., and L. K. Legatski. 1977. Venturi scrubbers.
14. In P. N. Cheremisinoff and R. A. Young (Eds.), Air Pollution Control and Design Handbook. Part 2. New York: Marcel Dekker.
15. Bethea, R. M. 1978. Air Pollution Control Technology. New York: Van Nostrand Reinhold.
16. Buonicore, A. J. 1982. Wet scrubbers. In L. Theodore and A. J. Buonicore (Eds.), Air Pollution
17. Jayaram, Varalakshmi Jayaram. Effect of Selective Catalytic Reduction Unit on Emissions from an Auxiliary Engine on an Ocean-Going Vessel. Rep. N.p.: n.p., 2009. Print.

18. Lavanchy, V. M. H., et al. "Elemental carbon (EC) and black carbon (BC) measurements with a thermal method and an aethalometer at the high-alpine research station Jungfraujoch." Atmospheric Environment 33.17 (1999): 2759-2769.
19. Petzold, Andreas, and Markus Schönlinner. "Multi-angle absorption photometry—a new method for the measurement of aerosol light absorption and atmospheric black carbon." Journal of Aerosol Science 35.4 (2004): 421-441.
20. AVL." AVL Micro Soot Sensor. N.p., n.d. Web. 15 Nov. 2014."5012 Multiangle Absorption Photometer (MAAP)." 5012 Multiangle Absorption Photometer (MAAP). N.p., n.d. Web. 15 Nov. 2014
21. "Aethalometer Overview." Magee Scientific. N.p., n.d. Web. 15 Nov. 2014
22. Moosmüller, H., R. K. Chakrabarty, and W. P. Arnott. "Aerosol light absorption and its measurement: A review." Journal of Quantitative Spectroscopy and Radiative Transfer 110.11 (2009): 844-878.
23. James, R. "Method and system for enhancing salt water exhaust scrubber efficiency." U.S. Patent Application 13/185,999.
24. Johnson, K.C. University of California, Riverside 201